

A Reference Multiparameter Viscosity Equation for Propane with an Optimized Functional Form

G. Scalabrin^{a)} and P. Marchi

Dipartimento di Fisica Tecnica, Università di Padova, via Venezia 1, I-35131 Padova, Italy

R. Span

Thermodynamik und Energietechnik (ThEt), Universität Paderborn, D-33098 Paderborn, Germany

(Received 9 September 2005; accepted 18 January 2006; published online 6 September 2006)

A multiparameter viscosity equation for propane, valid in wide temperature and pressure ranges, was developed through an optimization technique for the functional form. The obtained results are very satisfactory, showing an average absolute deviation of 0.28% for the currently available 1024 primary data points. This is a significant improvement with respect to the reference equation available in the literature. As usual, both the development and the evaluation of the viscosity equation requires a highly accurate equation of state in order to convert the independent variables used for the experimental data, in most applications, (T, P) , into the independent variables of the viscosity equation, (T, ρ) . The heuristic technique used to develop the equation allows to select consistent data sets and thus it is a powerful tool for screening the available experimental data. The present limit for the accuracy achievable in the representation of the viscosity surface of a pure fluid is set by the uncertainty level of the experimental data rather than by the effectiveness of the proposed modeling method. © 2006 American Institute of Physics. [DOI: 10.1063/1.2213629]

Key words: multiparameter equations; propane; transport properties correlation techniques; viscosity.

CONTENTS

Nomenclature.....	1416
1. Introduction.....	1417
2. Procedure for Developing an Empirical Equation for Viscosity.....	1417
2.1. Fitting a Multiparameter Empirical Equation.....	1417
2.2. Bank of Terms.....	1417
3. Multiparameter Viscosity Equation for the Whole Surface.....	1417
3.1. Experimental Data.....	1417
3.2. Screening Procedure and Primary Data Sets.....	1419
3.3. Near Critical Region.....	1419
3.4. The New Equation for the Viscosity of Propane.....	1420
4. Validation of the New Viscosity Equation.....	1422
5. Behavior of the Viscosity Surface.....	1424
5.1. Representation of the Viscosity Surface on a T, η Plane.....	1424
5.2. Representation of the Viscosity Surface on a P, η Plane.....	1424
5.3. Discussion on the Validity Limits.....	1424

6. Comparison with the Conventional Equation.....	1424
7. Zero-Density Limit and Initial Density Dependence of the New Viscosity Equation.....	1426
7.1. Calculation of the Scaling Factors.....	1429
7.2. Calculation of Quasi-Experimental $\eta^{(0)}$ and B_{η}^* Values.....	1430
7.3. Comparison of Models and Experimental Data.....	1432
8. Tabulations of the Overall Representation.....	1441
9. Conclusions.....	1441
10. References.....	1441

List of Tables

1. Substance-specific parameters for the target fluid propane.....	1417
2. Summary of the data sets available for propane.....	1418
3. Parameters of Eq. (4).....	1420
4. Validity limits of Eq. (4).....	1420
5. Deviations of the new viscosity equation, Eq. (4), with respect to primary, secondary, and overall data in liquid, vapor, and supercritical regions. Data are within the Eq. (4) validity limits.....	1421
6. Variables and parameters of Eq. (7) for the locus of minima found along isobars,	

^{a)}Author to whom correspondence should be addressed; electronic mail: gscal@unipd.it
© 2006 American Institute of Physics.

according to the new viscosity equation, Eq. (4).....	1426
7. Statistical analysis of the representation of the experimental data set by Eq. (4) and by the conventional equation of Vogel <i>et al.</i> ¹²	1428
8. Coefficients for Eq. (11).....	1430
9. Deviations between values calculated from the viscosity equations and the selected data.....	1430
10. Viscosity of propane along the saturation line..	1432
11. Viscosity of propane in the single phase regions.....	1433

List of Figures

1. Distribution of the data selected as primary data.....	1419
2. Representation of experimental and generated data in the near critical region.....	1420
3. Deviations between primary experimental data in the liquid phase and values calculated from Eq. (4).....	1422
4. Deviations between primary experimental data in the vapor phase and values calculated from Eq. (4).....	1423
5. Deviations between primary experimental data in the supercritical region and values calculated from Eq. (4).....	1423
6. Deviations between all primary experimental data and values calculated from Eq. (4) shown in a P, T diagram. The size of the symbols indicates the deviation between the selected experimental data and corresponding values calculated from Eq. (4).....	1424
7. Deviations between Eq. (4) and all the experimental points in the primary data sets, divided in several temperature ranges. The plotted lines correspond to values calculated from the conventional equation by Vogel <i>et al.</i> ¹²	1425
8. Isobars and saturated-vapor line calculated from Eq. (4) and plotted in a T, η plane. Viscosity minima are predicted in the dense gas phase.....	1426
9. Isotherms and saturation curve calculated from Eq. (4) on a P, η plane.....	1426
10. Isotherms and saturation curve calculated from Eq. (4) on a P, η plane for the vapor phase close to the critical point.....	1427
11. Isotherms and saturated-vapor line calculated from Eq. (4) and plotted on a P, η plane in the low-density gas region.....	1427
12. Experimental data and viscosity values calculated from Eq. (4) along isotherms in the vapor region at $\rho < 4.41 \text{ kg m}^{-3}$	1429
13. Representation of the viscosity zero-density limit $\eta^{(0)}(T)$ from the equations and the available experimental data.....	1431

14. Representation of the viscosity initial density dependence $\eta^{(1)}(T)$ from the equations and the available experimental data.....	1431
15. Representation of the reduced second viscosity virial coefficient B_η^* from the equations and the available experimental data.....	1431

Nomenclature

Symbol	Description
a, b, c, d	Adjustable parameters
AAD	Average absolute deviation
B_η	Second viscosity virial coefficient
B_η^*	Reduced B_η
Bias	Bias
d, t, n	Adjustable parameters
g, h, c	Adjustable parameters
H_c	Pseudo-critical viscosity
\bar{n}	Vector of individual coefficients
M	Molar mass
MAD	Maximum average deviation
N	Number of primary data
N_A	Avogadro number
NPT	Number of data points
P	Pressure
R	Gas constant
T	Thermodynamic temperature
T^*	Reduced temperature
x	Symbolic variable
y	Symbolic variable
Greek	
ε/k	Energy scaling parameter
χ^2	Weighted sum of squares
Δ	Error deviation
η	Viscosity
$\eta^{(0)}$	Viscosity in the zero-density limit
$\eta^{(1)}$	Viscosity initial density dependence
ρ	Mass density
σ	Length scaling parameter
Ω_η	Collision integral
Subscripts	
c	At the critical point
calc	Calculated
conv	Conventional equation
dg	Dilute-gas
exp	Experimental
i, j	Indices
min	At the minimum point
r	Reduced
zd	At zero-density limit

1. Introduction

Propane (R290) is a fluid with a wide application range, whose utilizations, besides the basic chemical processes, include refrigeration. Both the thermodynamic and the transport properties of this fluid are of great interest due to its important engineering applications.

Examining the literature, the approaches devoted to the representation of the viscosity surface of a fluid can be roughly divided into two groups. The first one includes predictive or semipredictive models; some of them are founded on theoretical bases, as for instance the evaluation of collision integrals, or are based on the corresponding states theory.^{1–10} In many cases these techniques are able to estimate the property with an accuracy level sufficient for engineering calculations, though requiring a limited amount of experimental data.

A second group is composed of semitheoretically founded and totally heuristic models, that are able to achieve a high precision in the property representation. This group also includes the present state-of-the-art technique for the development of viscosity equations, which is based on the residual concept superimposing three parts: the dilute-gas term, the excess term, and the critical enhancement term.¹¹

In the following, equations of this type will be referred to as “conventional equations,” as an example, the present reference equation for propane was developed according to such format by Vogel *et al.*¹² Even if some functional forms obtained from theoretical analysis are included in these equations, the technique is mainly correlative and then it requires experimental data as evenly distributed as possible over the whole $\eta\rho T$ surface. Some difficulties in the regression procedure are also present, as evidenced by Scalabrin *et al.*¹³

As an alternative, the totally heuristic methods have been developed. These are strictly related to mathematical models with the characteristic of being universal function approximators, that are applied to get the analytical relation between dependent and independent variables directly from the experimental representation of the studied phenomenon. Some viscosity models pertaining to this group are based on the multilayer feedforward neural networks,^{14–17} on a combination of the extended corresponding states and the neural networks techniques,^{18,19} or on functional form optimization algorithms.¹³

In particular, the technique for optimizing the functional form of multiparameter equations of state, set up by Setzmann and Wagner,²⁰ has already been successfully applied to model the viscosity of R134a¹³ and it is here applied to the case of propane.

2. Procedure for Developing an Empirical Equation for Viscosity

2.1. Fitting a Multiparameter Empirical Equation

An empirical equation for the viscosity surface of a fluid can be written as $\eta = \eta(T, \rho, \bar{n})$, where \bar{n} represents the vector of the individual coefficients to be fitted.

TABLE 1. Substance-specific parameters for the target fluid propane

		Reference
M (kg mol ⁻¹)	0.044098	21
T_c (K)	369.825	21
P_c (MPa)	4.248	21
ρ_c (kg m ⁻³)	220.48	21
H_c (μPa s)	17.1045	—

The determination of an optimum set of coefficients \bar{n} for the empirical equation is obtained by minimizing a sum of squares calculated as follows:

$$\chi^2(\bar{n}) = \sum_{i=1}^N \left(\frac{\eta_{\text{exp}} - \eta_{\text{calc}}(\bar{n})}{\eta_{\text{exp}}} \right)_i^2 \quad (1)$$

where N is the total number of primary experimental points and the subscripts exp and calc stand for experimental and calculated values, respectively.

The minimization technique used for the present study is based on the algorithm developed by Setzmann and Wagner.²⁰ Starting from a bank of terms the algorithm determines the functional form which yields the best representation of the selected experimental data.

2.2. Bank of Terms

The bank of terms used in the optimization of the functional form, which is composed of a total of 162 terms, can be written as

$$\eta_r = \sum_{i=0}^5 \sum_{j=0}^{20} n_{ij} T_r^i \rho_r^j + \sum_{i=0}^5 \sum_{j=0}^5 n_{ij} T_r^i \rho_r^j e^{-\rho_r^{2/2}} \quad (2)$$

where:

$$\begin{aligned} T_r &= T/T_c \\ \rho_r &= \rho/\rho_c \\ \eta_r &= \ln(\eta/H_c + 1) \\ H_c &= \frac{M^{1/2} P_c^{2/3}}{R^{1/6} N_A^{1/3} T_c^{1/6}} \end{aligned} \quad (3)$$

For the target fluid propane the parameters involved in the former variable definitions are reported in Table 1.

Further parameters are the molar gas constant ($R = 8.314472 \text{ J mol}^{-1} \text{ K}^{-1}$), assumed from Mohr and Taylor,²² and the Avogadro number ($N_A = 6.0221353 \times 10^{23} \text{ mol}^{-1}$), assumed from Becker *et al.*²³

3. Multiparameter Viscosity Equation for the Whole Surface

3.1. Experimental Data

The viscosity data sets for propane which are available from the literature are presented in Table 2, together with

TABLE 2. Summary of the data sets available for propane

Ref.	First author	Phase ^a	NPT	T range (K)	P range (MPa)	Meas. method ^b	Class
Liquid							
24	Babb	l	5	303	200–1000	RB	II
25	Baron	l	18	325–353	3.4–55.1	CV	II
26	Bicher	l	16	298–348	2.8–34.5	RB	II
27	Carmichael	l	8	278	1.5–31.2	RC	I
28	Diller	l	60	90–300	1.7–31.5	TC	I
29	Giddings	l	51	278–344	0.7–55.2	CV	I
30	Huang	l	30	173–273	6.9–34.5	FC	I
31	Sage	l	36	311–361	1.4–13.8	RB	II
32	Smith	l	55	295–368	1.4–34.5	RB	II
33	Starling	l	83	294–361	1.4–55.1	CV	I
34	Strumpf	l	5	311	3.2–7.2	TC	I
35	Swift	l	29	88–363	0.3–3.9	FC	II
36	Swift	l	13	243–363	0.3–4.1	FC	II
37	van Wijk	l	8	304–324	16.1–99.0	FN	II
28	Diller	sl	24	90–300	*	TC	I
38	Galkov	sl	5	112–176	*	CV	II
39	Gerf	sl	14	84–170	*	CV	II
30	Huang	sl	6	173–273	*	FC	I
40	Lipkin	sl	9	200–289	*	CV	II
31	Sage	sl	4	311–361	*	RB	II
Total		479					
Vapor							
41	Abe	v	5	298–468	0.1	OD	II
42	Abe	v	6	298–468	0.1	OD	II
43	Adzumi	v	8	303–373	0.1	C	II
25	Baron	v	6	325–408	0.7–3.4	CV	II
26	Bicher	v	3	398–498	2.8	RB	II
27	Carmichael	v	22	278–478	0.1–3.6	RC	II
44	Comings	v	35	303–378	0.1–4.2	CV	II
45	Diaz Pena	v	11	304–408	0.1	C	II
46	Diaz Pena	v	1	373	0.1	C	II
29	Giddings	v	14	278–378	0.1–4.1	CV	II
47	Hurly	v	11	298	0.1–0.8	GAV	II
48	Kestin	v	2	296–303	0.1	OD	I
49	Kestin	v	5	299–478	0.1	OD	II
50	Klemenc	v	1	273	0.1	C	II
51	Lambert	v	7	308–364	0.1	C	II
52	Nagaoka	v	3	298–348	0.1	RB	II
31	Sage	v	42	311–378	0.1–4.1	RB	II
53	Senftleben	v	1	313	0.1	HT	II
32	Smith	v	32	313–463	0.7–4.1	RB	II
33	Starling	v	30	294–411	0.7–4.1	CV	II
54	Titani	v	6	293–393	0.1	C	II
55	Trautz	v	6	301–549	0.1	C	II
56	Trautz	v	6	291–524	0.1	C	II
57	Vogel	v	70	297–626	0.0–0.3	OD	I
58	Wilhelm ^c	v	446	298–423	0.1–4.2	VW	I
59	Wobser	v	5	293–371	0.1	RB	I
31	Sage	sv	3	328–361	*	RB	II
Total		787					
Supercritical region							
25	Baron	sc	16	380–408	6.9–55.1	CV	II
26	Bicher	sc	21	398–498	4.8–34.5	RB	II

TABLE 2. Summary of the data sets available for propane—Continued

Ref.	First author	Phase ^a	NPT	T range (K)	P range (MPa)	Meas. method ^b	Class
27	Carmichael	sc	19	378–478	7.0–34.6	RC	I
29	Giddings	sc	13	378	5.5–55.2	CV	I
31	Sage	sc	9	378	4.5–13.8	RB	II
32	Smith	sc	24	388–463	5.2–34.5	RB	II
33	Starling	sc	39	378–411	5.5–55.1	CV	I
36	Swift	sc	1	370	4.3	FC	II
37	van Wijk	sc	12	374–423	36.8–145	FN	II
58	Wilhelm	sc	163	373–423	4.3–20.7	VW	I
Total			317				

Overall**Overall****1583**

^aPhase: l=liquid, sl=saturated liquid, v=vapor, sv=saturated vapor, sc=supercritical region.

^bMeasurement method: C=calculated, CV=capillary viscometer, FC=falling cylinder viscometer, FN=falling needle viscometer, GAV=Greenspan acoustic viscometer, HT=heat transfer between concentric cylinders, OD=oscillating disk viscometer, RB=rolling ball viscometer, RC=rotating cylinder viscometer, TC=torsional crystal viscometer, VW=vibrating wire viscometer.

^cFrom the Wilhelm and Vogel data set⁵⁸ five points at low-density conditions were skipped, because according to the authors they are affected by slip effect.

their temperature and pressure ranges. The meaning of the column denoted by “Class” will be explained in the following subsection.

3.2. Screening Procedure and Primary Data Sets

The available experimental data from the literature have been screened according to the following procedure.

Since for propane a viscosity equation in the conventional format was available from the literature,¹² this was used to screen the data within the validity range of that equation. All the available data were considered, including also those not assumed for the conventional equation development since they were published afterwards. An error threshold with respect to this equation was conventionally selected at an average absolute deviation (AAD) of 5%. Each data set was evaluated as a whole, because it was supposed that all the data from each set were obtained with a homogeneous accuracy. The data from this first screening compose the preliminary sources.

The preliminary data were obtained including also the points of the preliminary sources which fall outside the validity range of the conventional viscosity equation.

A first regression with the optimization algorithm was based on the preliminary data. A first selection of primary data sets was obtained considering only data with a threshold of 2%–3% for the AAD and a low value of the Bias.

A further screening of these data was carried out through regressions with the optimization algorithm refining the choice of the so called primary data sets. During this procedure some sets were moved from primary to secondary, and vice versa, searching for the AAD values of the single sets to be as similar as possible to the overall value for the primary data and for the Bias values close to zero.

The aim of the procedure was to gather sets with the low-

est error deviations and statistically centered as much as possible with respect to the multiparameter viscosity equation.

The screening finally led to a stable selection of primary data on which the final version of the multiparameter equation was regressed. In Table 2 and in the following tables the column “Class” reports the classification of the sets: the primary data sets are denoted by the symbol I, whereas the secondary by II. The distribution of the primary data on the P, T plane is shown in Fig. 1.

3.3. Near Critical Region

For propane no thermodynamic critical enhancement model has been published up to now and then no critical enhancement model for viscosity is available. Anyway, the influence of the critical enhancement for viscosity is limited

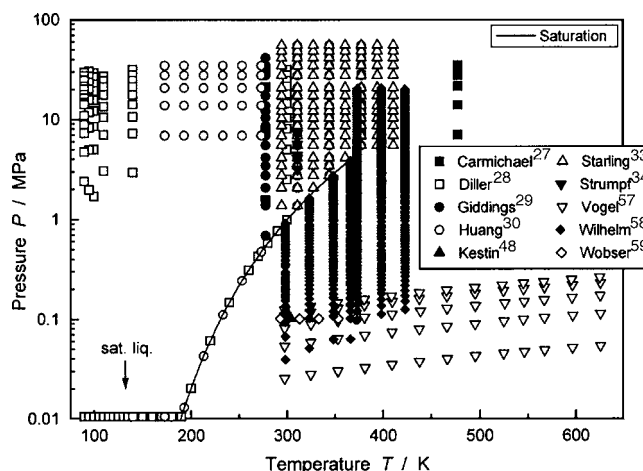


FIG. 1. Distribution of the data selected as primary data.

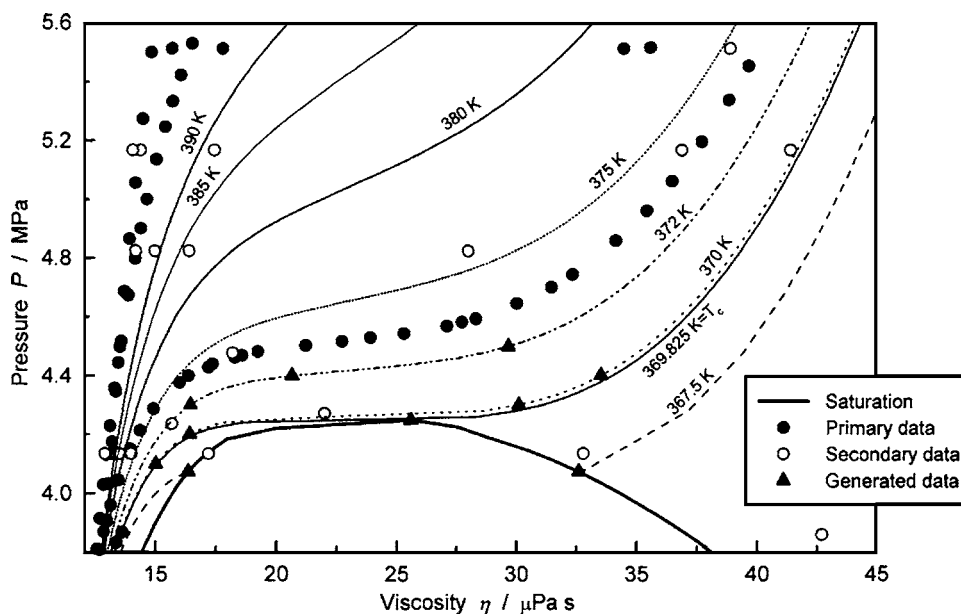


FIG. 2. Representation of experimental and generated data in the near critical region.

to a very narrow region centered on the critical point where viscosity presents an infinity limit.⁶⁰ In this work the modeling of a critical enhancement has been omitted as for the majority of the literature dedicated to viscosity equations.

In the near critical region data are anyway needed for the heuristic modeling procedure to let the new equation follow the characteristic trend close to the critical region as shown in Fig. 2. In that region no data are available from the literature and for this reason some data have been generated by the conventional viscosity equation of Vogel *et al.*¹² for a total of ten points distributed as in Fig. 2, where isotherms and saturation curve are from the conventional equation.¹² The goal of this integration is only to obtain a correct trend but not to assure a documented accuracy for the equation in the near critical region.

These data have then been used as primary data for the regression of the new viscosity multiparameter equation.

TABLE 3. Parameters of Eq. (4)

<i>i</i>	<i>t_i</i>	<i>d_i</i>	<i>n_i</i>
1	0.00	1.00	-0.7548580 × 10 ⁻¹
2	0.00	2.00	0.7607150
3	0.00	3.00	-0.1665680
4	0.00	13.00	0.1627612 × 10 ⁻⁵
5	1.00	12.00	0.1443764 × 10 ⁻⁴
6	1.00	16.00	-0.2759086 × 10 ⁻⁶
7	2.00	0.00	-0.1032756
8	2.00	18.00	-0.2498159 × 10 ⁻⁷
9	2.00	20.00	0.4069891 × 10 ⁻⁸
10	3.00	13.00	-0.1513434 × 10 ⁻⁵
11	4.00	4.00	0.2591327 × 10 ⁻²
12	1.00	0.00	0.5650076
13	2.00	1.00	0.1207253

3.4. The New Equation for the Viscosity of Propane

Given the final choice of the primary data sets, the following equation in the form $\eta = \eta(T, \rho)$ was obtained from the optimization procedure:

$$\eta_r = \sum_{i=1}^{11} n_i \cdot T_r^{t_i} \cdot \rho_r^{d_i} + e^{-\rho_r^{2/2}} \cdot \sum_{i=12}^{13} n_i \cdot T_r^{t_i} \cdot \rho_r^{d_i} \quad (4)$$

The coefficients and the exponents of Eq. (4) are reported in Table 3.

The validity limits of Eq. (4) are reported in Table 4. The extrapolation of the equation outside these validity limits, particularly at low temperatures and at high pressures, is not accurate and it could result in rather unreliable values.

As shown in Fig. 1, the primary data do not regularly fill all the regions of the stated validity range, but we chose to assume a contour as regular as possible for the validity range itself. This assumption will be discussed further on in Sec. 5.3.

The conversion from the experimental variables (*T, P*) to the equation variables (*T, ρ*) has been obtained using the dedicated equation of state (EoS) of Span and Wagner⁶¹ for propane.

TABLE 4. Validity limits of Eq. (4)

		Region
		Vapor and supercritical
<i>T</i> (K)	210–625	90–370
<i>P</i> (MPa)	≤ 100	≤ 100

TABLE 5. Deviations of the new viscosity equation, Eq. (4), with respect to primary, secondary, and overall data in liquid, vapor, and supercritical regions. Data are within the Eq. (4) validity limits.

Ref.	First author	Phase	NPT	T range (K)	P range (MPa)	Meas. method	AAD (%)	Bias (%)	MAD (%)	Class	
Liquid											
27	Carmichael	1	8	278	1.5–31.2	RC	0.47	0.01	0.95	I	
28	Diller	1	60	90–300	1.7–31.5	TC	0.83	-0.07	2.41	I	
29	Giddings	1	51	278–344	0.7–55.2	CV	0.42	0.32	1.57	I	
30	Huang	1	30	173–273	6.9–34.5	FC	0.39	-0.13	1.19	I	
33	Starling	1	83	294–361	1.4–55.1	CV	0.34	-0.13	1.29	I	
34	Strumpf	1	5	311	3.2–7.2	TC	0.73	0.35	1.22	I	
28	Diller	sl	24	90–300	*	TC	0.54	0.09	1.63	I	
30	Huang	sl	6	173–273	*	FC	0.32	0.31	0.66	I	
Primary		267				0.50		0.01		—	
25	Baron	1	18	325–353	3.4–55.1	CV	2.55	-2.13	5.35	II	
26	Bicher	1	16	298–348	2.8–34.5	RB	1.95	0.95	3.48	II	
31	Sage	1	36	311–361	1.4–13.8	RB	1.64	-0.01	4.87	II	
32	Smith	1	55	295–368	1.4–34.5	RB	3.65	0.58	22.02	II	
35	Swift	1	28	93–363	0.3–3.9	FC	4.52	1.94	12.50	II	
36	Swift	1	13	243–363	0.3–4.1	FC	2.09	-0.67	4.95	II	
37	van Wijk	1	8	304–324	16.1–99.0	FN	2.65	-1.80	3.98	II	
38	Galkov	sl	5	112–176	*	CV	1.73	-1.63	4.30	II	
39	Gerf	sl	10	90–170	*	CV	6.22	0.92	19.26	II	
40	Lipkin	sl	9	200–289	*	CV	7.00	7.00	11.41	II	
31	Sage	sl	4	311–361	*	RB	3.11	3.11	6.72	II	
Total		469				1.69		0.25		—	
Vapor											
48	Kestin	v	2	296–303	0.1	OD	0.28	0.28	0.30	I	
57	Vogel	v	70	297–626	0.0–0.3	OD	0.20	0.03	0.74	I	
58	Wilhelm	v	446	298–423	0.1–4.2	VW	0.11	-0.02	0.55	I	
59	Wobser	v	5	293–371	0.1	RB	0.19	0.01	0.30	I	
Primary		523				0.12		-0.01		—	
41	Abe	v	5	298–468	0.1	OD	0.49	0.49	1.01	II	
42	Abe	v	6	298–468	0.1	OD	0.48	0.48	0.94	II	
43	Adzumi	v	8	303–373	0.1	C	2.66	2.66	3.11	II	
25	Baron	v	6	325–408	0.7–3.4	CV	1.69	0.49	5.06	II	
26	Bicher	v	3	398–498	2.8	RB	6.29	2.83	13.68	II	
27	Carmichael	v	22	278–478	0.1–3.6	RC	1.03	0.94	4.30	II	
44	Comings	v	35	303–378	0.1–4.2	CV	1.59	0.02	11.99	II	
45	Diaz Pena	v	11	304–408	0.1	C	2.40	2.40	3.25	II	
46	Diaz Pena	v	1	373	0.1	C	3.22	3.22	3.22	II	
29	Giddings	v	14	278–378	0.1–4.1	CV	1.80	1.07	4.94	II	
47	Hurly	v	11	298	0.1–0.8	GAV	0.54	-0.54	0.81	II	
49	Kestin	v	5	299–478	0.1	OD	0.65	0.65	0.85	II	
50	Klemenc	v	1	273	0.1	C	1.14	1.14	1.14	II	
51	Lambert	v	7	308–364	0.1	C	2.46	2.46	2.66	II	
52	Nagaoka	v	3	298–348	0.1	RB	2.00	2.00	2.30	II	
31	Sage	v	42	311–378	0.1–4.1	RB	12.22	11.65	30.77	II	
53	Senftleben	v	1	313	0.1	HT	0.85	0.85	0.85	II	
32	Smith	v	32	313–463	0.7–4.1	RB	4.88	1.88	47.12	II	
33	Starling	v	30	294–411	0.7–4.1	CV	2.30	2.30	4.41	II	
54	Titani	v	6	293–393	0.1	C	1.63	1.63	2.33	II	
55	Trautz	v	6	301–549	0.1	C	1.18	-1.18	1.87	II	
56	Trautz	v	6	291–524	0.1	C	0.79	-0.68	1.75	II	
31	Sage	sv	3	328–361	*	RB	34.92	34.92	36.49	II	

TABLE 5. Deviations of the new viscosity equation, Eq. (4), with respect to primary, secondary, and overall data in liquid, vapor, and supercritical regions. Data are within the Eq. (4) validity limits.—Continued

Ref.	First author	Phase	NPT	T range (K)	P range (MPa)	Meas. method	AAD (%)	Bias (%)	MAD (%)	Class
			Total	787			1.46	1.07	—	
Supercritical region										
27	Carmichael	sc	19	378–478	7.0–34.6	RC	0.46	0.01	1.90	I
29	Giddings	sc	13	378	5.5–55.2	CV	0.47	0.37	1.45	I
33	Starling	sc	39	378–411	5.5–55.1	CV	0.64	0.34	3.20	I
58	Wilhelm	sc	163	373–423	4.3–20.7	VW	0.32	-0.26	4.41	I
			Primary	234			0.39	-0.10	—	
25	Baron	sc	16	380–408	6.9–55.1	CV	2.02	-0.82	5.93	II
26	Bicher	sc	21	398–498	4.8–34.5	RB	4.51	3.95	13.29	II
31	Sage	sc	9	378	4.5–13.8	RB	9.12	6.38	24.20	II
32	Smith	sc	24	388–463	5.2–34.5	RB	7.75	-7.46	16.84	II
36	Swift	sc	1	370	4.3	FC	26.15	-26.15	26.15	II
37	van Wijk	sc	8	374–423	36.8–97.8	FN	2.61	-2.19	4.78	II
			Total	313			1.70	-0.38	—	
Generated data										
Near critical generated data			10				2.57	2.57	3.81	
Overall										
Overall primary			1024				0.28	-0.02	—	
Overall			1569				1.58	0.54	—	

4. Validation of the New Viscosity Equation

The new viscosity equation has been validated in details with respect to both primary and secondary data. The results are reported in the following.

The deviations with respect to primary data and to data generated in the near critical region, given in Table 5 and Figs. 3–5, are considered as remaining deviations of the regression because the equation was regressed on these data. All the other data were not included in the regression.

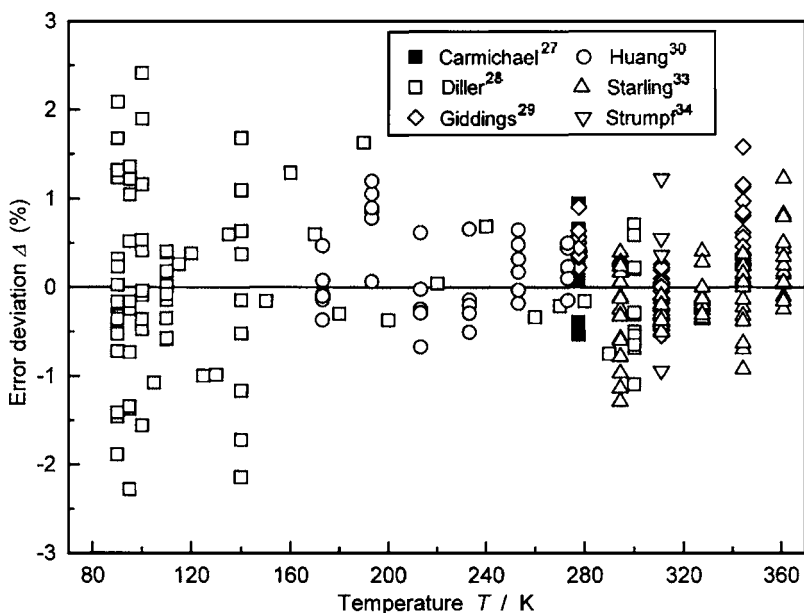


FIG. 3. Deviations between primary experimental data in the liquid phase and values calculated from Eq. (4).

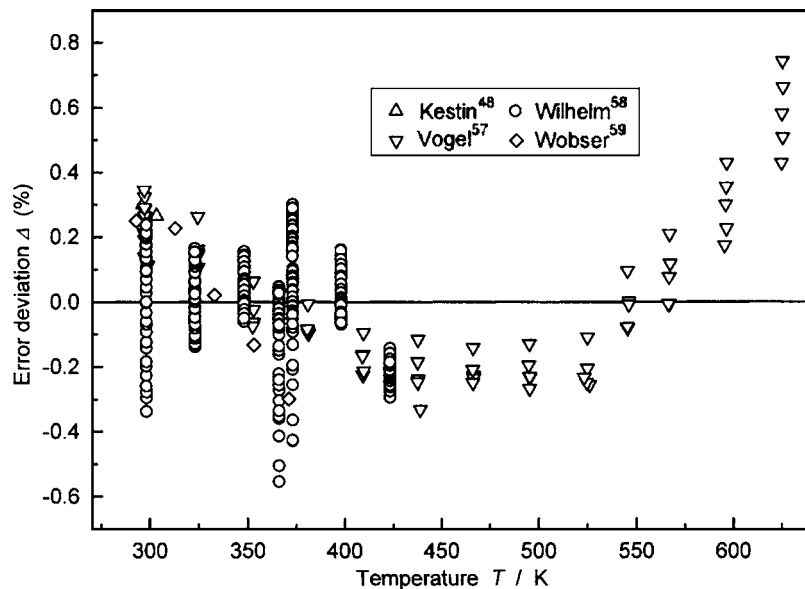


FIG. 4. Deviations between primary experimental data in the vapor phase and values calculated from Eq. (4).

The error deviation Δ has been calculated through all the present work as:

$$\text{Bias}(\%) = \frac{100}{NPT} \sum_{i=1}^{NPT} (\Delta)_i \quad (6)$$

$$\Delta = \frac{\eta_{\text{exp}} - \eta_{\text{calc}}}{\eta_{\text{exp}}} \quad (5)$$

From the error deviation Δ the following statistical quantities are evaluated: the average absolute deviation (AAD), the bias (Bias), and the maximum absolute deviation (MAD). These are calculated as:

$$\text{AAD}(\%) = \frac{100}{NPT} \sum_{i=1}^{NPT} |\Delta|_i$$

$$\text{MAD}(\%) = 100 \text{ Max}|\Delta|_i$$

The deviations of the new viscosity equation from primary data are shown in a P, T diagram in Fig. 6. The high precision of the equation is evidenced, particularly in the vapor region. Furthermore, in Fig. 7 the deviations of Eq. (4) with respect to all the experimental points of the primary data sets are represented as a function of pressure for several steps of temperature. The lines show the error deviation of Eq. (4) with respect to the conventional equation;¹² for each figure the temperature of the comparison between the two equations was taken at the mean value of the indicated range.

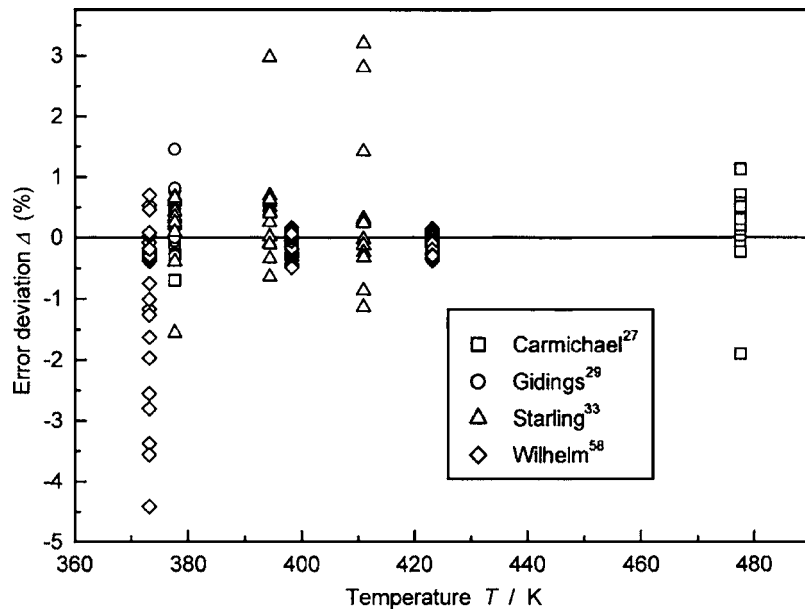


FIG. 5. Deviations between primary experimental data in the supercritical region and values calculated from Eq. (4).

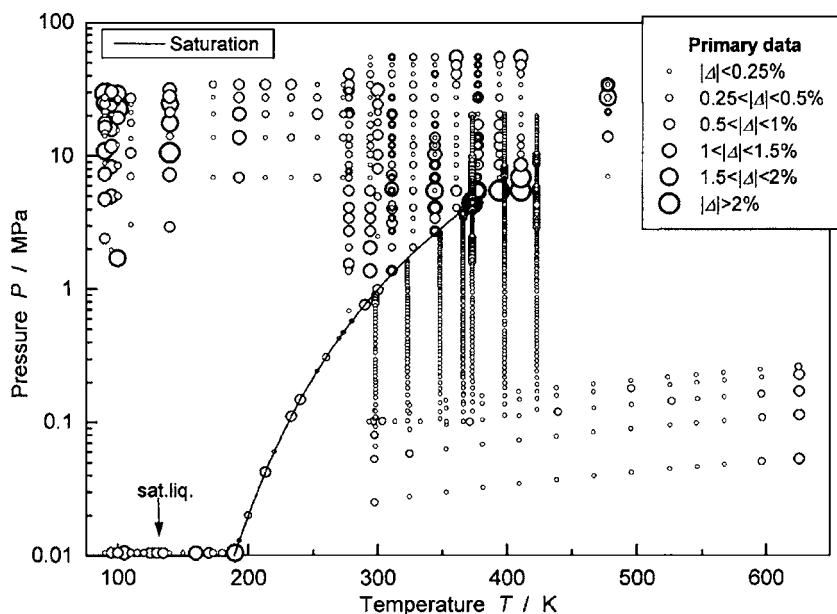


FIG. 6. Deviations between all primary experimental data and values calculated from Eq. (4) shown in a P, T diagram. The size of the symbols indicates the deviation between the selected experimental data and corresponding values calculated from Eq. (4).

5. Behavior of the Viscosity Surface

5.1. Representation of the Viscosity Surface on a T, η Plane

Some isobars in the gas phase and the vapor side of the saturation curve obtained from the new viscosity equation are plotted on a T, η plane in Fig. 8. A line of viscosity minima in the dense-gas region is observed. As it can be seen from Fig. 8, the viscosity minima were found in the pressure range $2.56 \leq P/\text{MPa} \leq 19$, corresponding to $0.60 \leq \eta_r \leq 4.47$. At higher pressures, the minimum is shifted to temperatures beyond the temperature range in which Eq. (4) is valid. The locus of the minima can be represented by functions in the form

$$y = a + bx + cx^2 + dx^3 \quad (7)$$

for which the variables and the corresponding parameters are reported in Table 6.

5.2. Representation of the Viscosity Surface on a P, η Plane

Plots of isotherms calculated from Eq. (4) on a P, η plane are shown in Fig. 9. In Fig. 10 a magnified part in the region of vapor close to the critical point is shown. The surface has a reasonable shape in that region and the trend of isotherms close to the critical one is correct.

The plot of isotherms calculated from Eq. (4) in the region of low-density vapor is shown in Fig. 11, together with the deviations of the equation from the primary experimental points. In the plot no evident viscosity minima are verified, being the isotherms represented with monotone lines.

5.3. Discussion on the Validity Limits

As from the brief discussion about the validity limits of the viscosity equation in Sec. 3.4, the preceding plots show that the primary data do not uniformly fill a single regular range, both in temperature and in pressure. For the sake of precision, an irregular contour for the validity range should be selected. But, looking at the plots reporting sections of the new equation together with experimental points, in particular at Figs. 9 and 11, it is evident that the trends of the new equation in the zones where experimental points are not available are regular and they correspond to the expected behavior. This indicates that the equation can be used also in these areas, taking into account that there the accuracy of the equation cannot be verified for lack of experimental data.

In fact in Fig. 9 one can see for instance a total lack of data for liquid states at $T < 270$ K and $P > 35$ MPa, whereas Fig. 11 shows that the data for vapor condition are not available for $T < 292$ K. Anyway, at liquid conditions even a strong increase of pressure scarcely increases the density of the fluid, thus the independent variable of the equation, the density, is moderately extrapolated; moreover, at low temperatures the gas densities are small enough to extrapolate the few terms composing the zero-density limit, assuming that the extrapolation behavior is reasonable (see Sec. 7).

However, slightly increased uncertainties may occur when the equation is applied, within the limits of the range of validity given in Table 5, in areas where there are no primary data available for comparisons.

6. Comparison with the Conventional Equation

The conventional equation of Vogel *et al.*¹² is used for comparison; the density required for this equation is cal-

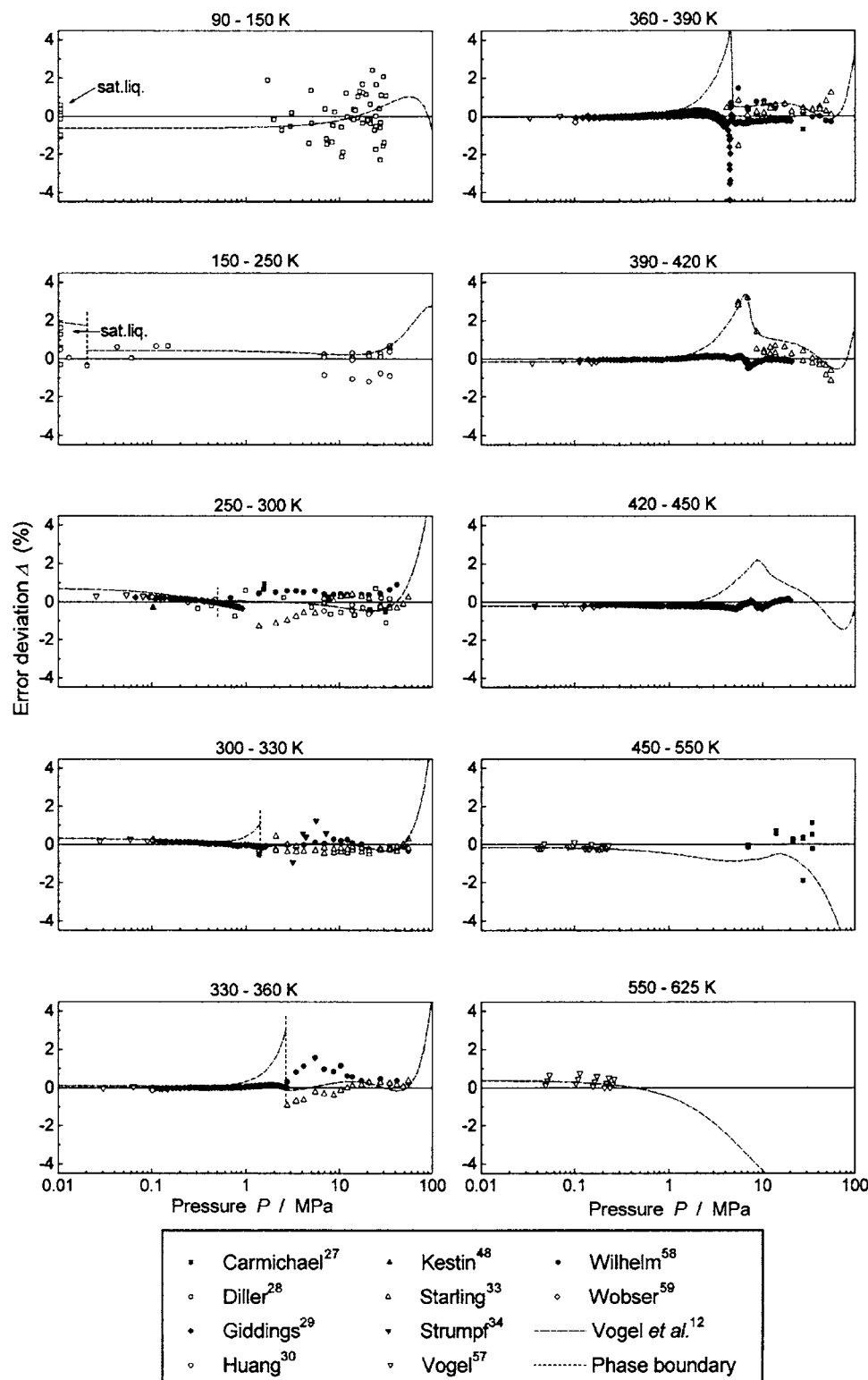


FIG. 7. Deviations between Eq. (4) and all the experimental points in the primary data sets, divided in several temperature ranges. The plotted lines correspond to values calculated from the conventional equation by Vogel *et al.*¹²

culated by the MBWR EoS from Younglove and Ely²¹ as in the original publication. The results are reported in Table 7.

With respect to primary data, the new viscosity equation, Eq. (4), is superior to the conventional equation for both the single phase regions and the whole surface, as the AAD and Bias values show.

A large difference is found for the vapor and the supercritical primary data: the present equation has an excellent behavior but the conventional one is shifted with respect to the data. For the conventional equation development, a reduced number of data was available for these regions and consequently the accuracy of that equation with respect to the present data base is lower.

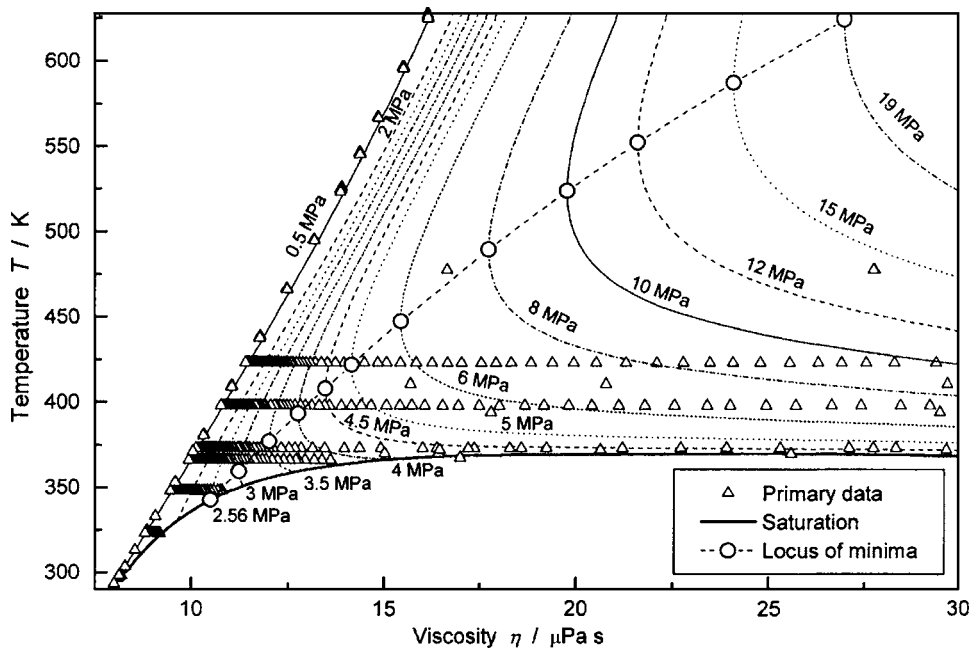


FIG. 8. Isobars and saturated-vapor line calculated from Eq. (4) and plotted in a T, η plane. Viscosity minima are predicted in the dense gas phase.

TABLE 6. Variables and parameters of Eq. (7) for the locus of minima found along isobars, according to the new viscosity equation, Eq. (4)

x	y	a	b	c	d
P_r	T_r	0.6478416	0.5325447	-0.1086438	0.009301453
P_r	ρ_r	0.1365860	0.2846208	-0.05167443	0.004736878
P_r	η_r	0.3213277	0.2993816	-0.05770175	0.004938074

7. Zero-Density Limit and Initial Density Dependence of the New Viscosity Equation

The literature presents some analysis of the viscosity behavior for the dilute-gas region which is in part theoretically founded; a comparison with those models^{12,62,63} is the aim of the present section. Both the present equation and the available experimental data have to be reduced in the basic format of that literature to allow a comparison.

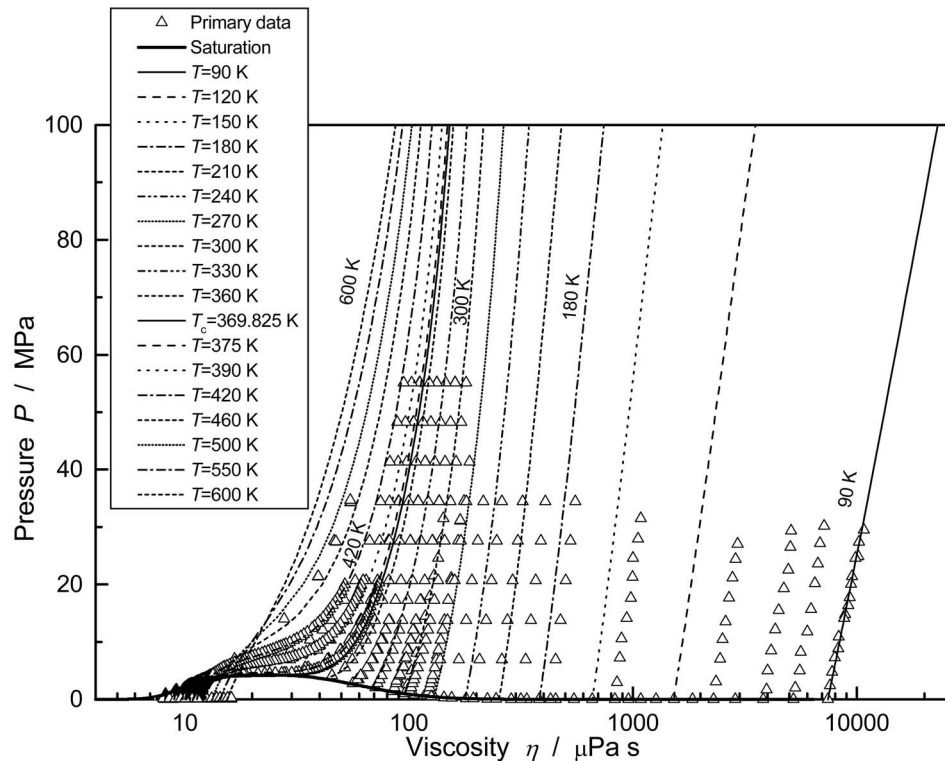


FIG. 9. Isotherms and saturation curve calculated from Eq. (4) on a P, η plane.

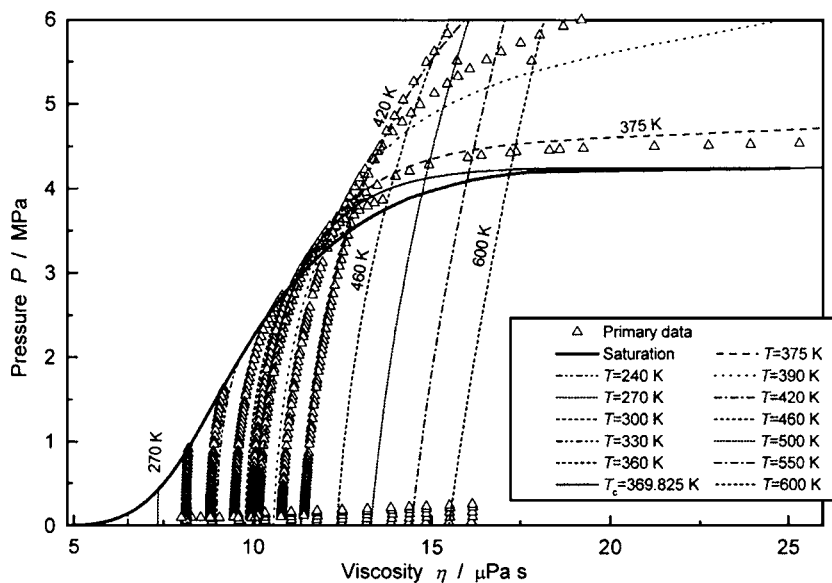


FIG. 10. Isotherms and saturation curve calculated from Eq. (4) on a P, η plane for the vapor phase close to the critical point.

It has been arbitrarily chosen to limit the dilute-gas region at the density value of 0.10 mol L^{-1} , i.e., 4.41 kg m^{-3} . A total of 150 primary points is available in the selected range $210 \leq T/K \leq 625$ and $\rho \leq 4.41 \text{ kg m}^{-3}$. The data and the behavior of the viscosity equation in such a region are represented in Fig. 12; each experimental point is indicated with the respective deviation from Eq. (4).

The dilute-gas viscosity predicted by an equation in the form $\eta = \eta(T, \rho)$ can be described through a Taylor series expansion in density around $\rho=0$, that is:

$$\begin{aligned}\eta(T, \rho) = & \left. \eta \right|_{\rho=0} + \left. \frac{\partial \eta}{\partial \rho} \right|_{\rho=0} \cdot \rho + \dots = \eta^{(0)}(T) + \eta^{(1)}(T)\rho \\ & + \dots = \eta^{(0)}(T)[1 + B_n(T)\rho + \dots]\end{aligned}\quad (8)$$

where $\eta^{(0)}$, $\eta^{(1)}$, and $B_\eta(T)$ are the zero-density limit, the initial density dependence, and the second viscosity virial

coefficient, respectively, they depend on temperature only.

Expanding the viscosity multiparameter Eq. (4) according to the truncated series of Eq. (8), the following two expressions are obtained:

$$\eta^{(0)}(T) = H_c(e^{n_7 T_r^2 + n_{12} T_r} - 1) \quad (9)$$

$$\eta^{(1)}(T) = \frac{H_c}{\rho_c} (n_1 + n_{13} T_r^2) \cdot e^{n_7 T_r^2 + n_{12} T_r}. \quad (10)$$

The coefficients for Eqs. 9 and 10 are the same reported in Table 3.

However, Eq. (9) represents the extrapolation of the viscosity surface at the physical condition of zero pressure, even if it cannot be experimentally verified exactly at this condition.

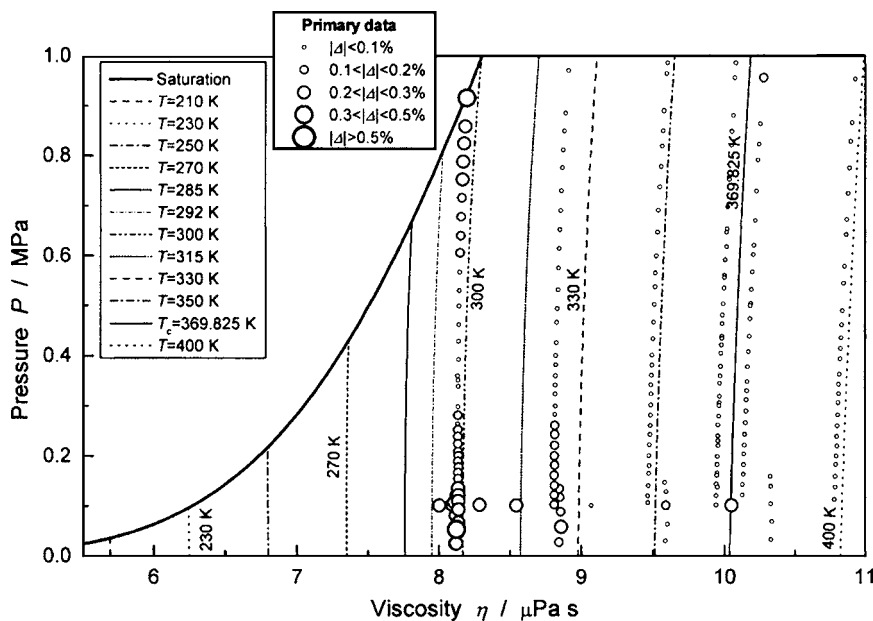


FIG. 11. Isotherms and saturated-vapor line calculated from Eq. (4) and plotted on a P, η plane in the low-density gas region.

TABLE 7. Statistical analysis of the representation of the experimental data set by Eq. (4) and by the conventional equation of Vogel *et al.*¹²

Ref.	First author	Phase	NPT	Eq. (4)			Vogel <i>et al.</i> ¹²			Class Eq. (4)
				AAD (%)	Bias (%)	MAD (%)	AAD (%)	Bias (%)	MAD (%)	
Liquid										
27	Carmichael	1	8	0.47	0.01	0.95	0.32	0.27	0.93	I
28	Diller	1	60	0.83	-0.07	2.41	0.84	-0.03	2.41	I
29	Giddings	1	51	0.42	0.32	1.57	0.45	0.38	1.51	I
30	Huang	1	30	0.39	-0.13	1.19	0.36	-0.20	1.60	I
33	Starling	1	83	0.34	-0.13	1.29	0.38	-0.15	1.29	I
34	Strumpf	1	5	0.73	0.35	1.22	0.72	0.36	1.21	I
28	Diller	sl	24	0.54	0.09	1.63	0.66	0.27	1.47	I
30	Huang	sl	6	0.32	0.31	0.66	0.25	0.08	0.39	I
Primary				267	0.50	0.01	—	0.52	0.04	—
25	Baron	1	18	2.55	-2.13	5.35	2.47	-2.15	5.43	II
26	Bicher	1	16	1.95	0.95	3.48	2.13	0.98	3.62	II
31	Sage	1	36	1.64	-0.01	4.87	1.72	-0.14	4.45	II
32	Smith	1	55	3.65	0.58	22.02	3.55	0.56	22.02	II
35	Swift	1	28	4.52	1.94	12.50	4.30	1.98	12.08	II
36	Swift	1	14	2.09	-0.67	4.95	2.00	-0.74	4.39	II
37	van Wijk	1	8	2.65	-1.80	3.98	2.99	-2.99	3.84	II
38	Galkov	sl	5	1.73	-1.63	4.30	1.21	-1.18	3.67	II
39	Gerf	sl	9	6.22	0.92	19.26	6.28	1.23	19.33	II
40	Lipkin	sl	9	7.00	7.00	11.41	6.80	6.80	11.38	II
31	Sage	sl	4	3.11	3.11	6.72	3.07	3.07	6.10	II
Total				469	1.69	0.25	—	1.68	0.24	—
Vapor										
48	Kestin	v	2	0.28	0.28	0.30	0.05	-0.05	0.05	I
57	Vogel	v	70	0.20	0.03	0.74	0.06	-0.03	0.21	I
58	Wilhelm	v	446	0.11	-0.02	0.55	0.65	-0.64	4.47	I
59	Wobser	v	5	0.19	0.01	0.30	0.14	-0.14	0.26	I
Primary				523	0.12	-0.01	—	0.56	-0.55	—
41	Abe	v	5	0.49	0.49	1.01	0.48	0.48	0.87	II
42	Abe	v	6	0.48	0.48	0.94	0.52	0.52	0.79	II
43	Adzumi	v	8	2.66	2.66	3.11	2.54	2.54	2.92	II
25	Baron	v	6	1.69	0.49	5.06	1.47	-0.11	2.91	II
26	Bicher	v	3	6.29	2.83	13.68	5.75	2.81	12.84	II
27	Carmichael	v	22	1.03	0.94	4.30	0.76	0.75	2.37	II
44	Comings	v	35	1.59	0.02	11.99	1.60	-0.66	8.78	II
45	Diaz Pena	v	11	2.40	2.40	3.25	2.34	2.34	3.31	II
46	Diaz Pena	v	1	3.22	3.22	3.22	3.26	3.26	3.26	II
29	Giddings	v	14	1.80	1.07	4.94	1.09	0.23	5.41	II
47	Hurly	v	11	0.54	-0.54	0.81	0.73	-0.73	0.99	II
49	Kestin	v	5	0.65	0.65	0.85	0.65	0.65	0.91	II
50	Klemenc	v	1	1.14	1.14	1.14	0.68	0.68	0.68	II
51	Lambert	v	7	2.46	2.46	2.66	2.35	2.35	2.58	II
52	Nagaoka	v	3	2.00	2.00	2.30	1.80	1.80	1.97	II
31	Sage	v	42	12.22	11.65	30.77	11.52	10.91	28.18	II
53	Senftleben	v	1	0.85	0.85	0.85	0.60	0.60	0.60	II
32	Smith	v	32	4.88	1.88	47.12	4.56	1.14	43.87	II
33	Starling	v	30	2.30	2.30	4.41	1.35	1.35	2.72	II
54	Titani	v	6	1.63	1.63	2.33	1.53	1.53	2.08	II
55	Trautz	v	6	1.18	-1.18	1.87	1.14	-1.14	1.67	II
56	Trautz	v	6	0.79	-0.68	1.75	0.66	-0.66	1.62	II
31	Sage	sv	3	34.92	34.92	36.49	32.95	32.95	33.90	II

TABLE 7. Statistical analysis of the representation of the experimental data set by Eq. (4) and by the conventional equation of Vogel *et al.*¹²—Continued

Ref.	First author	Phase	NPT	Eq. (4)			Vogel <i>et al.</i> ¹²			Class Eq. (4)
				AAD (%)	Bias (%)	MAD (%)	AAD (%)	Bias (%)	MAD (%)	
		Total	787	1.46	1.07	—	1.64	0.54	—	
Supercritical										
27	Carmichael	sc	19	0.46	0.01	1.90	0.66	-0.05	1.89	I
29	Giddings	sc	13	0.47	0.37	1.45	0.24	-0.04	0.93	I
33	Starling	sc	39	0.64	0.34	3.20	0.49	-0.40	2.09	I
58	Wilhelm	sc	163	0.32	-0.26	4.41	1.92	-1.92	7.73	I
		Primary	234	0.39	-0.10	—	1.49	-1.41	—	
25	Baron	sc	16	2.02	-0.82	5.93	2.11	-1.30	5.41	II
26	Bicher	sc	21	4.51	3.95	13.29	4.38	3.59	10.95	II
31	Sage	sc	9	9.12	6.38	24.20	8.49	5.15	20.86	II
32	Smith	sc	24	7.75	-7.46	16.84	8.43	-8.43	17.85	II
36	Swift	sc	1	26.15	-26.15	26.15	28.89	-28.89	28.89	II
37	van Wijk	sc	8	2.61	-2.19	4.78	2.46	-2.46	4.87	II
		Total	313	1.70	-0.38	—	2.56	-1.54	—	
Overall										
Overall primary		1024	0.28	-0.02	—	0.76	-0.59	—	—	
Overall		1569	1.58	0.54	—	1.83	0.03	—	—	

tion. Therefore, when the mean free path of the gas is comparable to the dimensions of the confining medium the viscosity equation is intended not to be valid.⁶⁴

7.1. Calculation of the Scaling Factors

The comparison of Eq. (4) with experimental data and with models from the literature, which are conceived in a unified reduced format, requires the calculation of the

fluid-specific scaling factors ε/k and σ . These are the energy and the length scaling parameters, respectively, which in the literature are used to make the models dimensionless and suitable to different fluids. The values of these parameters have to be regressed from viscosity experimental data in the dilute-gas region; in this work it was necessary to update the values for propane, published by Vogel *et al.*,¹² in order to consider the more recent data as well.

For such purposes an equation specific for the dilute-gas

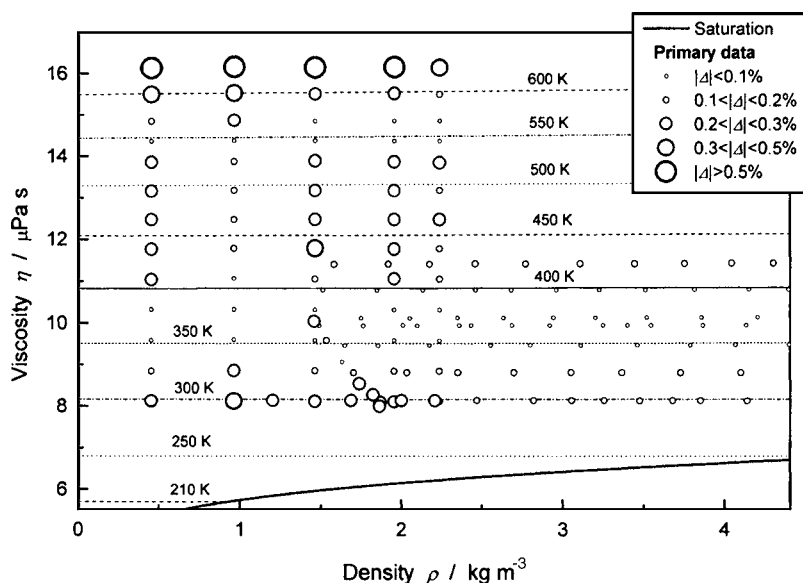


FIG. 12. Experimental data and viscosity values calculated from Eq. (4) along isotherms in the vapor region at $\rho < 4.41 \text{ kg m}^{-3}$.

TABLE 8. Coefficients for Eq. (11)

<i>i</i>	<i>g_i</i>	<i>h_i</i>	<i>c_i</i>
1	1	0	0.5947468
2	1	1	-4.333014
3	1.5	1	7.853046
4	2	1	-3.412503
5	4.5	0	-0.01062820
6	6	0	0.002142285

region has been developed from only the experimental data previously selected as primary and with $\rho \leq 4.41 \text{ kg m}^{-3}$; the obtained dilute-gas equation is:

$$\eta_{r,\text{dg}} = \frac{\eta}{H_c} = \sum_{i=1}^6 c_i T_r^{g_i} \rho_r^{h_i} \quad (11)$$

where the subscript dg denotes the dilute-gas condition; the numerical values of the coefficients and exponents of the equation are reported in Table 8.

The deviations of the viscosity equation, Eq. (4), of the dilute-gas equation, Eq. (11), and of the conventional equation of Vogel *et al.*¹² from the dilute-gas data are reported in Table 9.

The comparison in Table 9 shows that a lower AAD and Bias closer to zero are obtained for Eq. (11), specialized for the dilute-gas region, with respect to Eq. (4); also the overall AAD value of the conventional equation is slightly better than Eq. (4), but the values are below the best experimental uncertainty that can be reached with modern techniques. In particular the conventional equation in the vapor region was mainly regressed on the Vogel data⁵⁷ and then it has an excellent representation of such data, as it can be also seen in Table 7; on the other hand, its performance with respect to the recent and precise data set of Wilhelm and Vogel⁵⁸ shows a lower quality when moving to higher pressures (see Table 7). On the contrary, the new multiparameter viscosity equation, Eq. (4), has more homogeneous performances.

At the zero-density limit, the Taylor series expansion of Eq. (11) provides the following equations:

$$\eta_{\text{dg}}^{(0)}(T) = H_c(c_1 T_r + c_5 T_r^{4.5} + c_6 T_r^6) \quad (12)$$

$$\eta_{\text{dg}}^{(1)}(T) = \frac{H_c}{\rho_c}(c_2 T_r + c_3 T_r^{1.5} + c_4 T_r^2) \quad (13)$$

for which the coefficients are in Table 8.

Once these equations have been obtained, the scaling factors ε/k_B and σ , necessary in the following developments, can be determined. In the conventional equation the dilute-gas term $\eta_{\text{conv}}^{(0)}$ [Eq. (4) from Vogel *et al.*¹²], derived from the kinetic theory of gases, is given in a generalized form and it is normally adapted to the target fluid by fitting the scaling factors ε/k_B and σ on suitable experimental data extrapolated to zero density. The procedure adopted in the present work aims at getting the values of these parameters by forcing the equation $\eta_{\text{conv}}^{(0)}$ to be as close as possible to the corresponding Eq. (12), which was obtained from only experimental data. Furthermore, the same equation and coefficients a_i as those of the conventional equation [Eq. (5) from Vogel *et al.*¹²] were assumed for the collision integral Ω_η included in the cited $\eta_{\text{conv}}^{(0)}$ relation. Greater details about the fitting procedure are given in the corresponding Sec. 7.1 of the work from Scalabrin *et al.*¹³ The values $\varepsilon/k_B = 266.076 \text{ K}$ and $\sigma = 0.4967 \text{ nm}$ have been obtained from the fitting.

These values have been used for processing the experimental data and for plotting the equations derived from both Eqs. (4) and (11), remembering that the reduced second viscosity virial coefficient B_η^* and the reduced temperature T^* are defined as:¹²

$$B_\eta^* = \frac{M}{N_A \sigma^3} \cdot \frac{\eta^{(1)}}{\eta^{(0)}} \quad (14)$$

$$T^* = \frac{kT}{\varepsilon} \quad (15)$$

7.2. Calculation of Quasi-Experimental $\eta^{(0)}$ and B_η^* Values

In order to allow a comparison of the experimental data with the models available for this region, a data reduction is needed to convert the data into the same format generating quasi-experimental values. Only the primary data with ρ

TABLE 9. Deviations between values calculated from the viscosity equations and the selected data

Ref.	First author	NPT	Eq. (4)			Eq. (11)			Vogel <i>et al.</i> ¹²		
			AAD (%)	Bias (%)	MAD (%)	AAD (%)	Bias (%)	MAD (%)	AAD (%)	Bias (%)	MAD (%)
48	Kestin	2	0.28	0.28	0.30	0.05	0.05	0.05	0.05	-0.05	0.05
57	Vogel	70	0.20	0.03	0.74	0.04	0.00	0.14	0.06	-0.03	0.21
58	Wilhelm	73	0.09	0.00	0.24	0.03	0.00	0.10	0.06	-0.02	0.14
59	Wobser	5	0.19	0.01	0.30	0.10	-0.08	0.23	0.14	-0.14	0.26
Overall primary		150	0.15	0.02	0.74	0.04	0.00	0.23	0.06	-0.03	0.26

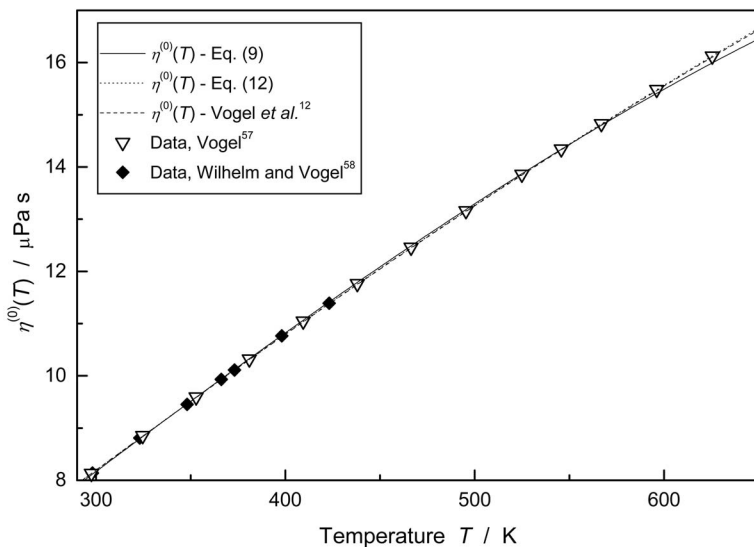


FIG. 13. Representation of the viscosity zero-density limit $\eta^{(0)}(T)$ from the equations and the available experimental data.

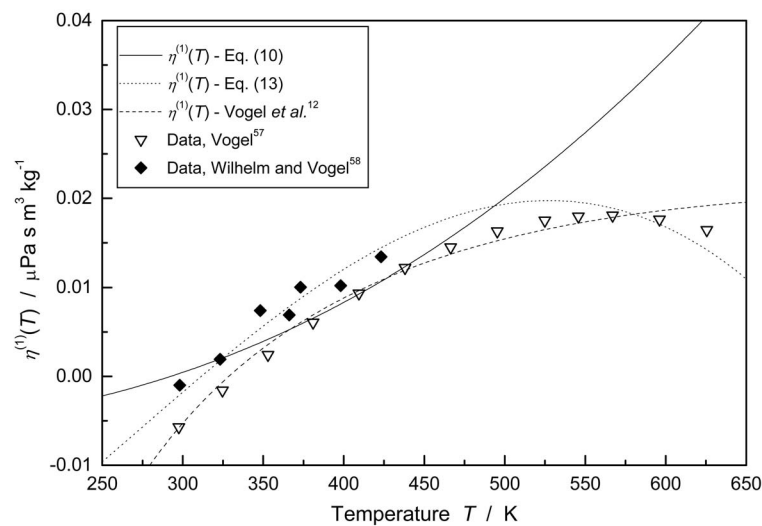


FIG. 14. Representation of the viscosity initial density dependence $\eta^{(1)}(T)$ from the equations and the available experimental data.

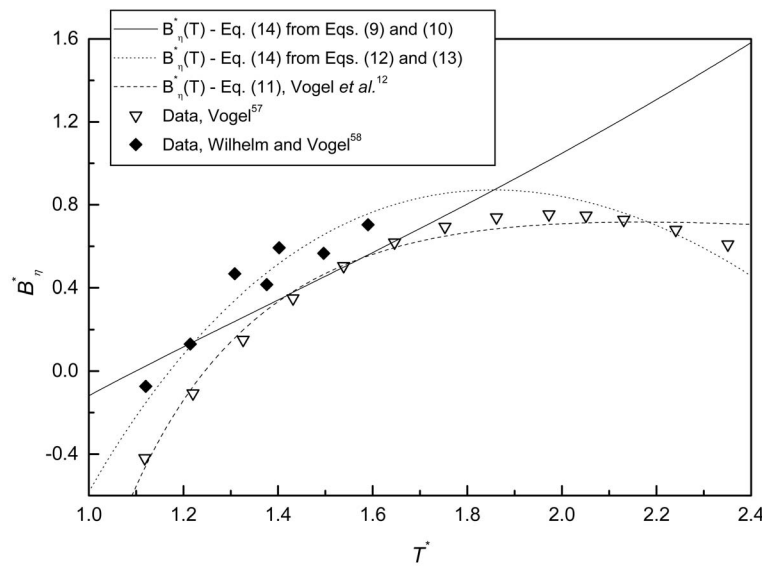


FIG. 15. Representation of the reduced second viscosity virial coefficient B_{η}^* from the equations and the available experimental data.

TABLE 10. Viscosity of propane along the saturation line

Temperature (K)	Pressure (MPa)	Saturated liquid		Saturated vapor	
		Density (kg m ⁻³)	Viscosity (μPa s)	Density (kg m ⁻³)	Viscosity (μPa s)
90.0	9.718×10^{-10}	731.47	7416.0	5.723×10^{-8}	2.4015
95.0	5.440×10^{-9}	725.83	5184.3	3.037×10^{-7}	2.5374
100.0	2.447×10^{-8}	720.28	3799.6	1.298×10^{-6}	2.6734
105.0	9.817×10^{-8}	714.80	2894.9	4.959×10^{-6}	2.8097
110.0	3.425×10^{-7}	709.40	2277.6	1.651×10^{-5}	2.9461
115.0	1.059×10^{-6}	704.05	1840.4	4.885×10^{-5}	3.0827
120.0	2.950×10^{-6}	698.76	1520.7	1.304×10^{-4}	3.2195
125.0	7.501×10^{-6}	693.50	1280.4	3.183×10^{-4}	3.3564
130.0	1.760×10^{-5}	688.28	1095.4	7.182×10^{-4}	3.4934
135.0	3.849×10^{-5}	683.08	949.97	1.512×10^{-3}	3.6306
140.0	7.904×10^{-5}	677.90	833.44	2.995×10^{-3}	3.7679
145.0	1.535×10^{-4}	672.74	738.55	5.616×10^{-3}	3.9053
150.0	2.836×10^{-4}	667.59	660.13	0.010032	4.0429
155.0	5.010×10^{-4}	662.44	594.49	0.017157	4.1805
160.0	8.502×10^{-4}	657.29	538.89	0.028214	4.3181
165.0	1.391×10^{-3}	652.13	491.29	0.044791	4.4558
170.0	2.203×10^{-3}	646.96	450.16	0.068878	4.5936
175.0	3.385×10^{-3}	641.77	414.30	0.10291	4.7314
180.0	5.062×10^{-3}	636.57	382.81	0.14978	4.8691
185.0	7.384×10^{-3}	631.34	354.93	0.21289	5.0069
190.0	0.010530	626.07	330.11	0.29610	5.1446
195.0	0.014707	620.77	307.87	0.40381	5.2823
200.0	0.020154	615.43	287.83	0.54086	5.4198
205.0	0.027140	610.05	269.68	0.71261	5.5574
210.0	0.035962	604.61	253.17	0.92486	5.6948
215.0	0.046949	599.12	238.08	1.1839	5.8322
220.0	0.060458	593.57	224.24	1.4964	5.9696
225.0	0.076872	587.95	211.49	1.8696	6.1069
230.0	0.096600	582.25	199.72	2.3112	6.2443
235.0	0.12008	576.48	188.80	2.8292	6.3818
240.0	0.14775	570.61	178.65	3.4324	6.5196
245.0	0.18011	564.65	169.19	4.1299	6.6578
250.0	0.21764	558.59	160.35	4.9316	6.7965
255.0	0.26085	552.41	152.06	5.8481	6.9359
260.0	0.31027	546.11	144.28	6.8908	7.0765
265.0	0.36645	539.68	136.95	8.0720	7.2184
270.0	0.42993	533.09	130.04	9.4054	7.3622
273.0	0.47176	529.07	126.08	10.285	7.4495
275.0	0.50128	526.35	123.50	10.906	7.5083
280.0	0.58108	519.43	117.31	12.590	7.6574
285.0	0.66993	512.31	111.43	14.477	7.8102
290.0	0.76843	504.98	105.83	16.587	7.9678
295.0	0.87719	497.41	100.49	18.945	8.1312
298.0	0.94764	492.75	97.399	20.491	8.2327
300.0	0.99686	489.58	95.380	21.580	8.3020
305.0	1.1281	481.44	90.474	24.524	8.4818
310.0	1.2715	472.97	85.749	27.819	8.6729
315.0	1.4278	464.11	81.183	31.511	8.8782
320.0	1.5978	454.81	76.751	35.663	9.1010
325.0	1.7822	444.99	72.429	40.349	9.3463
330.0	1.9818	434.55	68.191	45.669	9.6202
335.0	2.1974	423.38	64.006	51.754	9.9314
340.0	2.4301	411.29	59.839	58.789	10.292
345.0	2.6808	398.03	55.647	67.039	10.721
350.0	2.9507	383.20	51.365	76.921	11.247

TABLE 10. Viscosity of propane along the saturation line—Continued

Temperature (K)	Pressure (MPa)	Saturated liquid		Saturated vapor	
		Density (kg m ⁻³)	Viscosity (μPa s)	Density (kg m ⁻³)	Viscosity (μPa s)
355.0	3.2414	366.09	46.891	89.147	11.924
360.0	3.5546	345.25	42.024	105.14	12.862
365.0	3.8928	316.52	36.201	128.80	14.376

<4.41 kg m⁻³ have been considered; moreover, the Kestin *et al.*⁴⁸ and the Wobser and Müller⁵⁹ data are too few for the present purpose and they were rejected.

The data set from Wilhelm and Vogel⁵⁸ presents viscosity values measured along seven isothermal lines; therefore each of them was fitted as a function of density with a straight line, whose parameters are the $\eta^{(0)}$ and $\eta^{(1)}$ values at that temperature.

The data from Vogel⁵⁷ are not organized in isotherms, but it is possible to divide them into 13 quasi-isothermal groups. An equation similar to Eq. (11) was regressed for this data set and the corresponding $\eta^{(0)}$ and $\eta^{(1)}$ formulations were obtained according to Eq. (8); the evaluation of these last equations at the mean temperature of each quasi-isothermal group yielded the searched $\eta^{(0)}$ and $\eta^{(1)}$ values.

7.3. Comparison of Models and Experimental Data

In Figs. 13–15 the equations for $\eta^{(0)}$, $\eta^{(1)}$, and B_{η}^* derived from Eq. (4) are plotted together with the equations derived from dilute-gas Eq. (11), with the conventional equation,¹² and with the values from the experimental data.^{57,58}

In Fig. 13 for the zero-density limit a very good agreement between all the equations and the experimental data sets is shown. For the initial density dependence, Fig. 14 presents a situation of lower precision, because the present Eq. (10), derived from Eq. (4), does not correctly represent the data. In fact it does not basically follow the data trend, whereas the equation from Vogel *et al.*¹² looks both to follow the trend and to be validated.

For the reduced second viscosity virial coefficient B_{η}^* as shown in Fig. 15, the conventional equation from Vogel *et al.*¹² looks to correctly represent the data, the present dilute-gas equation, Eq. (11), in the same data range reaches a lower level of accuracy, while the new viscosity equation, Eq. (4), does not follow the data trend. It should be considered that the generalized correlation for B_{η}^* used in the conventional equation [Eq. (11) from Vogel *et al.*¹²] was in particular regressed for propane, as an enhancement of the Rainwater–Friend theory.^{62,63}

Looking at Table 9, the data sets of Vogel⁵⁷ and Wilhelm and Vogel⁵⁸ are represented with a very high accuracy from both Eqs. (4) and (11), even if these equations present appreciable deviations with respect to the same data sets when analyzing the plots in Figs. 14 and 15. The correct representation of viscosity in the dilute-gas region by the form $B_{\eta}^*(T^*)$ requires an extremely high accuracy level of the equation,

TABLE 11. Viscosity of propane in the single phase regions

Temperature	90 K		100 K		110 K	
	Pressure (MPa)	Density (kg m ⁻³)	Viscosity (μPa s)	Density (kg m ⁻³)	Viscosity (μPa s)	Density (kg m ⁻³)
0.01	731.48	7416.9	720.28	3800.0	709.40	2277.8
0.05	731.49	7420.5	720.29	3801.6	709.42	2278.7
0.10	731.51	7425.0	720.31	3803.7	709.44	2279.8
0.15	731.52	7429.5	720.33	3805.7	709.46	2280.9
0.20	731.54	7434.0	720.35	3807.8	709.48	2282.0
0.25	731.55	7438.5	720.36	3809.8	709.49	2283.2
0.30	731.57	7443.1	720.38	3811.9	709.51	2284.3
0.35	731.59	7447.6	720.40	3813.9	709.53	2285.4
0.40	731.60	7452.1	720.42	3816.0	709.55	2286.6
0.50	731.63	7461.1	720.45	3820.1	709.59	2288.8
0.60	731.67	7470.2	720.49	3824.2	709.63	2291.1
0.80	731.73	7488.3	720.56	3832.5	709.70	2295.6
1.00	731.79	7506.4	720.63	3840.8	709.78	2300.1
1.50	731.95	7551.9	720.80	3861.5	709.97	2311.4
2.00	732.11	7597.7	720.97	3882.3	710.15	2322.8
2.50	732.27	7643.7	721.15	3903.2	710.34	2334.2
3.00	732.43	7689.9	721.32	3924.2	710.53	2345.7
3.50	732.59	7736.3	721.49	3945.2	710.72	2357.2
4.00	732.75	7783.0	721.66	3966.4	710.90	2368.7
5.00	733.06	7877.0	722.00	4009.0	711.27	2391.9
6.00	733.37	7972.0	722.34	4051.9	711.64	2415.2
8.00	734.00	8164.8	723.02	4138.8	712.38	2462.4
10.00	734.62	8361.5	723.69	4227.2	713.10	2510.3
15.00	736.14	8870.6	725.34	4454.7	714.89	2632.9
20.00	737.64	9405.7	726.96	4691.9	716.63	2759.9
25.00	739.10	9968.1	728.54	4939.3	718.34	2891.6
30.00	740.54	10559.0	730.09	5197.4	720.01	3028.3
35.00	741.96	11181.0	731.62	5466.8	721.65	3170.1
40.00	743.35	11834.0	733.11	5747.9	723.25	3317.4
50.00	746.06	13244.0	736.02	6348.4	726.37	3629.5
60.00	748.69	14804.0	738.83	7004.3	729.37	3967.5
80.00	753.71	18447.0	744.19	8509.7	735.06	4734.0
100.00	758.46	22940.0	749.23	10328.	740.40	5649.0
Temperature	120 K		130 K		140 K	
Pressure (MPa)	Density (kg m ⁻³)	Viscosity (μPa s)	Density (kg m ⁻³)	Viscosity (μPa s)	Density (kg m ⁻³)	Viscosity (μPa s)
0.01	698.76	1520.8	688.28	1095.5	677.91	833.51
0.05	698.78	1521.4	688.30	1095.9	677.93	833.79
0.10	698.80	1522.1	688.32	1096.4	677.95	834.15
0.15	698.82	1522.8	688.34	1096.9	677.98	834.50
0.20	698.84	1523.5	688.37	1097.4	678.00	834.85
0.25	698.86	1524.2	688.39	1097.8	678.02	835.21
0.30	698.88	1524.9	688.41	1098.3	678.05	835.56
0.35	698.90	1525.6	688.43	1098.8	678.07	835.92
0.40	698.92	1526.3	688.45	1099.3	678.10	836.27
0.50	698.96	1527.7	688.50	1100.2	678.15	836.98
0.60	699.00	1529.1	688.54	1101.2	678.20	837.69
0.80	699.08	1531.9	688.63	1103.1	678.29	839.11
1.00	699.17	1534.8	688.72	1105.1	678.39	840.53
1.50	699.37	1541.8	688.95	1109.9	678.63	844.09
2.00	699.58	1548.9	689.17	1114.8	678.87	847.65
2.50	699.78	1556.0	689.39	1119.6	679.11	851.22
3.00	699.98	1563.1	689.61	1124.5	679.35	854.79

TABLE 11. Viscosity of propane in the single phase regions—Continued

Temperature	120 K		130 K		140 K	
	Pressure (MPa)	Density (kg m ⁻³)	Viscosity (μPa s)	Density (kg m ⁻³)	Viscosity (μPa s)	Density (kg m ⁻³)
3.50	700.19	1570.3	689.83	1129.4	679.59	858.37
4.00	700.39	1577.4	690.05	1134.3	679.83	861.96
5.00	700.79	1591.8	690.48	1144.1	680.30	869.16
6.00	701.19	1606.3	690.92	1154.0	680.77	876.39
8.00	701.98	1635.5	691.78	1173.8	681.70	890.92
10.00	702.77	1665.0	692.63	1193.9	682.62	905.57
15.00	704.70	1740.5	694.71	1245.0	684.87	942.72
20.00	706.58	1818.2	696.74	1297.4	687.06	980.68
25.00	708.42	1898.5	698.72	1351.3	689.18	1019.5
30.00	710.21	1981.3	700.64	1406.6	691.25	1059.2
35.00	711.97	2066.9	702.52	1463.6	693.26	1100.0
40.00	713.69	2155.4	704.36	1522.3	695.23	1141.9
50.00	717.01	2342.0	707.91	1645.5	699.01	1229.2
60.00	720.21	2542.6	711.31	1777.1	702.63	1322.0
80.00	726.26	2993.9	717.72	2071.3	709.41	1528.2
100.00	731.91	3528.5	723.69	2417.8	715.70	1769.8
Temperature	150 K		160 K		170 K	
Pressure (MPa)	Density (kg m ⁻³)	Viscosity (μPa s)	Density (kg m ⁻³)	Viscosity (μPa s)	Density (kg m ⁻³)	Viscosity (μPa s)
0.01	667.59	660.19	657.29	538.93	646.97	450.19
0.05	667.62	660.41	657.32	539.11	646.99	450.34
0.10	667.64	660.68	657.35	539.33	647.02	450.52
0.15	667.67	660.96	657.37	539.55	647.05	450.71
0.20	667.69	661.23	657.40	539.78	647.09	450.90
0.25	667.72	661.51	657.43	540.00	647.12	451.09
0.30	667.75	661.78	657.46	540.22	647.15	451.28
0.35	667.77	662.06	657.49	540.45	647.18	451.46
0.40	667.80	662.34	657.52	540.67	647.21	451.65
0.50	667.85	662.89	657.58	541.12	647.27	452.03
0.60	667.91	663.44	657.63	541.56	647.34	452.40
0.80	668.01	664.54	657.75	542.46	647.46	453.15
1.00	668.12	665.64	657.86	543.35	647.59	453.91
1.50	668.38	668.40	658.15	545.59	647.90	455.78
2.00	668.64	671.17	658.44	547.83	648.21	457.66
2.50	668.90	673.94	658.72	550.07	648.52	459.54
3.00	669.16	676.71	659.00	552.31	648.83	461.42
3.50	669.42	679.48	659.29	554.56	649.14	463.30
4.00	669.68	682.26	659.57	556.81	649.44	465.18
5.00	670.20	687.83	660.12	561.31	650.05	468.95
6.00	670.71	693.42	660.68	565.81	650.65	472.72
8.00	671.72	704.64	661.77	574.86	651.84	480.26
10.00	672.71	715.93	662.85	583.93	653.01	487.82
15.00	675.14	744.45	665.48	606.79	655.86	506.78
20.00	677.50	773.46	668.02	629.93	658.59	525.88
25.00	679.78	803.00	670.47	653.38	661.23	545.15
30.00	682.00	833.13	672.85	677.19	663.78	564.61
35.00	684.15	863.89	675.15	701.41	666.24	584.32
40.00	686.25	895.37	677.39	726.08	668.63	604.31
50.00	690.28	960.71	681.68	777.01	673.20	645.32
60.00	694.12	1029.8	685.75	830.48	677.51	688.05
80.00	701.29	1182.0	693.34	947.42	685.52	780.58
100.00	707.91	1359.5	700.30	1082.7	692.83	886.64

TABLE 11. Viscosity of propane in the single phase regions—Continued

Temperature	180 K		190 K		200 K	
	Pressure (MPa)	Density (kg m ⁻³)	Viscosity (μPa s)	Density (kg m ⁻³)	Viscosity (μPa s)	Density (kg m ⁻³)
0.01	636.57	382.82	0.28111	5.1447	0.26674	5.4209
0.05	636.60	382.95	626.10	330.22	615.46	287.91
0.10	636.63	383.11	626.14	330.37	615.50	288.04
0.15	636.67	383.28	626.18	330.51	615.54	288.17
0.20	636.70	383.44	626.22	330.66	615.58	288.30
0.25	636.74	383.60	626.25	330.80	615.63	288.43
0.30	636.77	383.76	626.29	330.94	615.67	288.56
0.35	636.81	383.93	626.33	331.09	615.71	288.69
0.40	636.84	384.09	626.37	331.23	615.75	288.82
0.50	636.91	384.41	626.44	331.52	615.83	289.08
0.60	636.98	384.74	626.52	331.81	615.92	289.34
0.80	637.12	385.39	626.67	332.38	616.08	289.86
1.00	637.25	386.04	626.82	332.96	616.25	290.38
1.50	637.60	387.66	627.19	334.40	616.66	291.68
2.00	637.94	389.28	627.57	335.83	617.07	292.98
2.50	638.27	390.91	627.94	337.27	617.48	294.28
3.00	638.61	392.53	628.31	338.70	617.88	295.57
3.50	638.95	394.15	628.67	340.14	618.29	296.86
4.00	639.28	395.77	629.04	341.57	618.69	298.15
5.00	639.94	399.01	629.76	344.43	619.48	300.73
6.00	640.60	402.25	630.48	347.28	620.26	303.30
8.00	641.89	408.73	631.89	352.99	621.80	308.43
10.00	643.16	415.21	633.27	358.67	623.31	313.53
15.00	646.24	431.40	636.61	372.84	626.93	326.19
20.00	649.19	447.62	639.79	386.96	630.38	338.73
25.00	652.03	463.90	642.85	401.06	633.67	351.20
30.00	654.76	480.27	645.78	415.15	636.81	363.59
35.00	657.40	496.76	648.60	429.28	639.83	375.95
40.00	659.94	513.41	651.32	443.47	642.73	388.30
50.00	664.80	547.32	656.48	472.16	648.23	413.06
60.00	669.38	582.35	661.33	501.51	653.36	438.13
80.00	677.83	657.35	670.24	563.51	662.74	490.29
100.00	685.50	742.28	678.29	632.72	671.18	547.51
Temperature	220 K		240 K		260 K	
Pressure (MPa)	Density (kg m ⁻³)	Viscosity (μPa s)	Density (kg m ⁻³)	Viscosity (μPa s)	Density (kg m ⁻³)	Viscosity (μPa s)
0.01	0.24209	5.9732	0.22168	6.5248	0.20448	7.0749
0.05	1.2317	5.9703	1.1228	6.5228	1.0325	7.0738
0.10	593.61	224.33	2.2838	6.5208	2.0916	7.0729
0.15	593.66	224.44	570.62	178.66	3.1792	7.0726
0.20	593.71	224.55	570.68	178.76	4.2980	7.0730
0.25	593.76	224.67	570.74	178.86	5.4509	7.0741
0.30	593.81	224.78	570.81	178.96	6.6412	7.0760
0.35	593.87	224.89	570.87	179.07	546.18	144.35
0.40	593.92	225.00	570.94	179.17	546.26	144.45
0.50	594.02	225.23	571.07	179.37	546.43	144.65
0.60	594.12	225.45	571.19	179.58	546.59	144.84
0.80	594.32	225.90	571.45	179.99	546.92	145.23
1.00	594.53	226.35	571.70	180.40	547.25	145.62
1.50	595.03	227.47	572.34	181.41	548.07	146.59
2.00	595.53	228.59	572.96	182.43	548.87	147.55
2.50	596.03	229.70	573.58	183.44	549.66	148.51

TABLE 11. Viscosity of propane in the single phase regions—Continued

Temperature	220 K		240 K		260 K	
	Pressure (MPa)	Density (kg m ⁻³)	Viscosity (μPa s)	Density (kg m ⁻³)	Viscosity (μPa s)	Density (kg m ⁻³)
3.00	596.52	230.81	574.19	184.44	550.44	149.46
3.50	597.01	231.92	574.80	185.45	551.22	150.41
4.00	597.50	233.03	575.40	186.45	551.98	151.35
5.00	598.46	235.23	576.58	188.43	553.47	153.23
6.00	599.40	237.42	577.74	190.41	554.93	155.08
8.00	601.26	241.78	580.00	194.32	557.74	158.73
10.00	603.06	246.10	582.19	198.18	560.42	162.32
15.00	607.36	256.74	587.34	207.62	566.68	171.05
20.00	611.41	267.18	592.13	216.80	572.39	179.46
25.00	615.23	277.45	596.60	225.75	577.65	187.58
30.00	618.87	287.56	600.81	234.48	582.54	195.45
35.00	622.33	297.53	604.78	243.01	587.12	203.09
40.00	625.63	307.39	608.55	251.36	591.43	210.50
50.00	631.84	326.83	615.57	267.58	599.36	224.70
60.00	637.59	346.07	622.01	283.27	606.55	238.18
80.00	647.99	384.75	633.51	313.65	619.26	263.36
100.00	657.24	425.40	643.62	343.96	630.28	287.09
Temperature	273 K		280 K		298 K	
Pressure (MPa)	Density (kg m ⁻³)	Viscosity (μPa s)	Density (kg m ⁻³)	Viscosity (μPa s)	Density (kg m ⁻³)	Viscosity (μPa s)
0.01	0.19467	7.4314	0.18978	7.6229	0.17825	8.1136
0.05	0.98159	7.4308	0.95626	7.6226	0.89693	8.1141
0.10	1.9845	7.4306	1.9316	7.6227	1.8084	8.1151
0.15	3.0101	7.4309	2.9272	7.6233	2.7351	8.1165
0.20	4.0601	7.4318	3.9442	7.6246	3.6778	8.1185
0.25	5.1362	7.4334	4.9842	7.6264	4.6373	8.1210
0.30	6.2405	7.4356	6.0487	7.6288	5.6146	8.1241
0.35	7.3754	7.4386	7.1395	7.6320	6.6104	8.1277
0.40	8.5435	7.4425	8.2587	7.6359	7.6260	8.1320
0.50	529.12	126.13	10.592	7.6462	9.7212	8.1425
0.60	529.33	126.32	519.47	117.35	11.911	8.1560
0.80	529.73	126.71	519.92	117.74	16.633	8.1935
1.00	530.13	127.10	520.37	118.13	492.91	97.507
1.50	531.11	128.06	521.47	119.10	494.45	98.528
2.00	532.08	129.01	522.55	120.05	495.94	99.533
2.50	533.03	129.96	523.60	121.00	497.39	100.52
3.00	533.96	130.90	524.64	121.94	498.80	101.50
3.50	534.88	131.84	525.66	122.88	500.17	102.46
4.00	535.78	132.76	526.66	123.80	501.51	103.41
5.00	537.55	134.60	528.60	125.63	504.09	105.28
6.00	539.26	136.41	530.49	127.44	506.55	107.11
8.00	542.54	139.98	534.08	130.98	511.16	110.65
10.00	545.66	143.46	537.46	134.43	515.42	114.08
15.00	552.82	151.89	545.18	142.74	524.90	122.22
20.00	559.25	159.96	552.06	150.67	533.13	129.89
25.00	565.12	167.73	558.29	158.28	540.43	137.19
30.00	570.53	175.21	564.00	165.59	547.02	144.17
35.00	575.55	182.44	569.28	172.65	553.04	150.87
40.00	580.25	189.43	574.21	179.46	558.60	157.31
50.00	588.84	202.75	583.17	192.38	568.61	169.47
60.00	596.57	215.24	591.21	204.46	577.46	180.73
80.00	610.10	238.12	605.20	226.37	592.70	200.74

TABLE 11. Viscosity of propane in the single phase regions—Continued

Temperature	273 K		280 K		298 K		
	Pressure (MPa)	Density (kg m ⁻³)	Viscosity (μPa s)	Density (kg m ⁻³)	Viscosity (μPa s)	Density (kg m ⁻³)	Viscosity (μPa s)
100.00	621.74	258.92	617.19	245.91	605.60	217.87	
Temperature	300 K		320 K		340 K		
	Pressure (MPa)	Density (kg m ⁻³)	Viscosity (μPa s)	Density (kg m ⁻³)	Viscosity (μPa s)	Density (kg m ⁻³)	Viscosity (μPa s)
0.01	0.17706	8.1680	0.16595	8.7095	0.15615	9.2467	
0.05	0.89080	8.1685	0.83393	8.7109	0.78401	9.2488	
0.10	1.7957	8.1696	1.6786	8.7129	1.5763	9.2518	
0.15	2.7155	8.1712	2.5343	8.7154	2.3771	9.2552	
0.20	3.6507	8.1732	3.4016	8.7183	3.1867	9.2590	
0.25	4.6022	8.1758	4.2809	8.7217	4.0053	9.2632	
0.30	5.5708	8.1789	5.1725	8.7255	4.8333	9.2678	
0.35	6.5574	8.1826	6.0772	8.7298	5.6708	9.2728	
0.40	7.5630	8.1870	6.9953	8.7347	6.5183	9.2783	
0.50	9.6357	8.1975	8.8742	8.7460	8.2444	9.2905	
0.60	11.799	8.2110	10.815	8.7596	10.014	9.3047	
0.80	16.451	8.2482	14.904	8.7946	13.698	9.3394	
1.00	489.59	95.387	19.325	8.8421	17.600	9.3837	
1.50	491.20	96.419	32.529	9.0414	28.596	9.5487	
2.00	492.75	97.434	456.87	77.726	42.349	9.8359	
2.50	494.26	98.433	459.32	78.899	412.02	60.087	
3.00	495.72	99.416	461.63	80.034	416.87	61.760	
3.50	497.15	100.39	463.84	81.136	421.18	63.294	
4.00	498.53	101.34	465.95	82.209	425.07	64.721	
5.00	501.20	103.22	469.90	84.277	431.93	67.336	
6.00	503.74	105.05	473.57	86.259	437.88	69.716	
8.00	508.49	108.61	480.20	90.015	447.93	74.000	
10.00	512.87	112.04	486.11	93.554	456.34	77.853	
15.00	522.59	120.17	498.64	101.74	473.03	86.365	
20.00	530.98	127.82	509.02	109.26	486.05	93.917	
25.00	538.42	135.09	517.96	116.32	496.86	100.88	
30.00	545.11	142.04	525.84	123.03	506.16	107.41	
35.00	551.23	148.71	532.92	129.43	514.38	113.62	
40.00	556.86	155.12	539.37	135.55	521.75	119.54	
50.00	566.99	167.21	550.80	147.07	534.63	130.64	
60.00	575.94	178.39	560.76	157.67	545.68	140.83	
80.00	591.32	198.24	577.63	176.24	564.11	158.61	
100.00	604.33	215.16	591.69	191.55	579.27	172.98	
Temperature	360 K		380 K		400 K		
	Pressure (MPa)	Density (kg m ⁻³)	Viscosity (μPa s)	Density (kg m ⁻³)	Viscosity (μPa s)	Density (kg m ⁻³)	Viscosity (μPa s)
0.01	0.14745	9.7788	0.13967	10.305	0.13267	10.825	
0.05	0.73981	9.7817	0.70040	10.309	0.66501	10.829	
0.10	1.4861	9.7857	1.4060	10.314	1.3342	10.835	
0.15	2.2391	9.7900	2.1168	10.319	2.0075	10.841	
0.20	2.9989	9.7947	2.8330	10.325	2.6852	10.848	
0.25	3.7656	9.7997	3.5546	10.330	3.3672	10.855	
0.30	4.5395	9.8051	4.2819	10.337	4.0536	10.862	
0.35	5.3207	9.8108	5.0148	10.343	4.7445	10.869	
0.40	6.1094	9.8170	5.7535	10.350	5.4399	10.877	
0.50	7.7102	9.8304	7.2488	10.365	6.8448	10.893	

TABLE 11. Viscosity of propane in the single phase regions—Continued

Temperature	360 K		380 K		400 K	
	Pressure (MPa)	Density (kg m ⁻³)	Viscosity (μPa s)	Density (kg m ⁻³)	Viscosity (μPa s)	Density (kg m ⁻³)
0.60	9.3433	9.8455	8.7688	10.381	8.2688	10.910
0.80	12.714	9.8809	11.887	10.418	11.177	10.949
1.00	16.238	9.9240	15.117	10.461	14.170	10.993
1.50	25.858	10.073	23.759	10.601	22.064	11.130
2.00	37.024	10.300	33.394	10.799	30.646	11.312
2.50	50.592	10.652	44.359	11.075	40.074	11.549
3.00	68.576	11.243	57.202	11.465	50.563	11.858
3.50	99.253	12.564	72.926	12.036	62.423	12.263
4.00	360.01	45.478	93.705	12.945	76.107	12.800
5.00	379.12	50.422	207.82	21.262	112.17	14.565
6.00	391.70	54.010	315.38	36.341	170.30	18.519
8.00	409.40	59.580	359.89	45.863	289.72	32.391
10.00	422.34	64.099	382.27	51.697	333.75	40.436
15.00	445.40	73.312	415.47	62.075	383.13	52.378
20.00	461.95	81.042	436.72	70.124	410.44	60.824
25.00	475.10	87.983	452.72	77.117	429.84	67.905
30.00	486.10	94.414	465.70	83.488	445.07	74.241
35.00	495.61	100.47	476.68	89.436	457.68	80.100
40.00	504.03	106.23	486.25	95.066	468.50	85.616
50.00	518.49	117.01	502.44	105.57	486.51	95.886
60.00	530.71	126.91	515.89	115.23	501.25	105.34
80.00	550.79	144.18	537.67	132.17	524.78	122.03
100.00	567.08	158.05	555.11	145.82	543.39	135.64
Temperature	420 K		440 K		460 K	
Pressure (MPa)	Density (kg m ⁻³)	Viscosity (μPa s)	Density (kg m ⁻³)	Viscosity (μPa s)	Density (kg m ⁻³)	Viscosity (μPa s)
0.01	0.12634	11.337	0.12059	11.841	0.11534	12.337
0.05	0.63305	11.342	0.60405	11.847	0.57761	12.344
0.10	1.2695	11.349	1.2108	11.855	1.1575	12.353
0.15	1.9093	11.356	1.8204	11.863	1.7396	12.362
0.20	2.5526	11.364	2.4328	11.872	2.3241	12.371
0.25	3.1993	11.371	3.0480	11.880	2.9108	12.380
0.30	3.8496	11.379	3.6661	11.889	3.4999	12.390
0.35	4.5035	11.388	4.2871	11.898	4.0914	12.400
0.40	5.1610	11.396	4.9109	11.907	4.6852	12.410
0.50	6.4871	11.414	6.1676	11.927	5.8800	12.431
0.60	7.8283	11.432	7.4363	11.947	7.0845	12.453
0.80	10.558	11.473	10.011	11.990	9.5233	12.499
1.00	13.352	11.519	12.637	12.038	12.003	12.549
1.50	20.649	11.655	19.440	12.176	18.389	12.690
2.00	28.445	11.828	26.617	12.344	25.062	12.857
2.50	36.820	12.044	34.212	12.547	32.045	13.052
3.00	45.876	12.311	42.274	12.788	39.366	13.278
3.50	55.738	12.639	50.864	13.075	47.052	13.539
4.00	66.562	13.044	60.044	13.412	55.134	13.837
5.00	91.908	14.167	80.469	14.276	72.602	14.562
6.00	123.92	15.929	104.14	15.465	91.975	15.491
8.00	209.19	22.695	162.01	19.234	136.55	18.113
10.00	276.98	30.978	223.56	24.836	185.62	21.846
15.00	348.75	44.161	313.53	37.511	279.58	32.507
20.00	383.42	52.944	356.15	46.380	329.34	41.064
25.00	406.68	60.095	383.53	53.515	360.76	48.044

TABLE 11. Viscosity of propane in the single phase regions—Continued

Temperature	420 K		440 K		460 K	
	Pressure (MPa)	Density (kg m ⁻³)	Viscosity (μPa s)	Density (kg m ⁻³)	Viscosity (μPa s)	Density (kg m ⁻³)
30.00	424.37	66.394	403.81	59.742	383.61	54.136
35.00	438.73	72.166	419.98	65.414	401.58	59.679
40.00	450.88	77.575	433.48	70.712	416.42	64.851
50.00	470.77	87.624	455.30	80.541	440.16	74.452
60.00	486.84	96.890	472.70	89.627	458.87	83.357
80.00	512.14	113.39	499.76	105.96	487.68	99.528
100.00	531.91	127.05	520.69	119.71	509.74	113.40
Temperature	480 K		500 K		520 K	
	Pressure (MPa)	Density (kg m ⁻³)	Viscosity (μPa s)	Density (kg m ⁻³)	Viscosity (μPa s)	Density (kg m ⁻³)
0.01	0.11053	12.822	0.10610	13.298	0.10202	13.762
0.05	0.55339	12.830	0.53114	13.306	0.51061	13.772
0.10	1.1087	12.840	1.0638	13.317	1.0225	13.783
0.15	1.6658	12.850	1.5981	13.328	1.5357	13.796
0.20	2.2248	12.860	2.1339	13.340	2.0502	13.808
0.25	2.7858	12.871	2.6713	13.351	2.5660	13.820
0.30	3.3486	12.881	3.2102	13.363	3.0831	13.833
0.35	3.9134	12.892	3.7508	13.374	3.6016	13.845
0.40	4.4801	12.903	4.2930	13.386	4.1213	13.858
0.50	5.6194	12.926	5.3821	13.410	5.1648	13.884
0.60	6.7666	12.949	6.4777	13.435	6.2136	13.911
0.80	9.0851	12.998	8.6885	13.488	8.3273	13.966
1.00	11.436	13.051	10.926	13.543	10.463	14.024
1.50	17.463	13.196	16.639	13.693	15.898	14.181
2.00	23.713	13.364	22.528	13.864	21.473	14.355
2.50	30.200	13.555	28.601	14.054	27.194	14.546
3.00	36.938	13.772	34.865	14.266	33.062	14.755
3.50	43.941	14.016	41.326	14.499	39.080	14.983
4.00	51.223	14.289	47.991	14.757	45.251	15.230
5.00	66.671	14.932	61.949	15.345	58.052	15.784
6.00	83.353	15.715	76.754	16.039	71.457	16.419
8.00	120.31	17.771	108.74	17.767	99.905	17.940
10.00	160.49	20.516	142.94	19.956	129.89	19.786
15.00	249.17	29.044	223.57	26.815	202.68	25.456
20.00	303.76	36.909	280.11	33.786	258.83	31.528
25.00	338.75	43.576	317.85	40.007	298.32	37.221
30.00	364.00	49.457	345.19	45.602	327.35	42.472
35.00	383.69	54.830	366.44	50.760	349.96	47.378
40.00	399.83	59.854	383.79	55.611	368.39	52.030
50.00	425.42	69.208	411.12	64.694	397.33	60.815
60.00	445.41	77.928	432.34	73.219	419.69	69.133
80.00	475.91	93.933	464.46	89.050	453.36	84.781
100.00	499.07	107.94	488.69	103.19	478.60	99.044
Temperature	540 K		560 K		580 K	
	Pressure (MPa)	Density (kg m ⁻³)	Viscosity (μPa s)	Density (kg m ⁻³)	Viscosity (μPa s)	Density (kg m ⁻³)
0.01	0.098237	14.215	0.094726	14.655	0.091457	15.081
0.05	0.49162	14.225	0.47399	14.666	0.45759	15.093
0.10	0.98431	14.238	0.94889	14.680	0.91594	15.108
0.15	1.4781	14.251	1.4247	14.694	1.3750	15.123

TABLE 11. Viscosity of propane in the single phase regions—Continued

Temperature	540 K		560 K		580 K	
	Pressure (MPa)	Density (kg m ⁻³)	Viscosity (μPa s)	Density (kg m ⁻³)	Viscosity (μPa s)	Density (kg m ⁻³)
0.20	1.9730	14.264	1.9014	14.708	1.8349	15.138
0.25	2.4689	14.277	2.3790	14.722	2.2955	15.154
0.30	2.9660	14.291	2.8575	14.737	2.7569	15.169
0.35	3.4641	14.304	3.3370	14.751	3.2190	15.185
0.40	3.9633	14.318	3.8173	14.766	3.6819	15.200
0.50	4.9651	14.346	4.7807	14.796	4.6100	15.232
0.60	5.9712	14.375	5.7478	14.826	5.5411	15.264
0.80	7.9968	14.433	7.6929	14.888	7.4123	15.330
1.00	10.040	14.495	9.6526	14.953	9.2956	15.398
1.50	15.227	14.658	14.616	15.123	14.057	15.575
2.00	20.527	14.836	19.671	15.306	18.892	15.765
2.50	25.942	15.030	24.818	15.504	23.801	15.967
3.00	31.473	15.239	30.056	15.714	28.783	16.180
3.50	37.119	15.464	35.385	15.938	33.836	16.405
4.00	42.882	15.704	40.804	16.176	38.958	16.642
5.00	54.751	16.235	51.901	16.692	49.402	17.149
6.00	67.062	16.830	63.326	17.260	60.093	17.700
8.00	92.846	18.213	87.018	18.549	82.086	18.923
10.00	119.71	19.836	111.47	20.019	104.61	20.286
15.00	185.72	24.673	171.82	24.268	160.25	24.114
20.00	240.06	29.953	223.69	28.899	209.47	28.232
25.00	280.35	35.100	263.99	33.527	249.21	32.397
30.00	310.60	39.972	295.00	38.012	280.57	36.507
35.00	334.32	44.598	319.58	42.342	305.76	40.540
40.00	353.69	49.031	339.73	46.543	326.53	44.500
50.00	384.08	57.493	371.39	54.662	359.26	52.264
60.00	407.49	65.593	395.75	62.531	384.48	59.894
80.00	442.60	81.045	432.20	77.777	422.16	74.922
100.00	468.81	95.424	459.31	92.264	450.11	89.510
Temperature	600 K		620 K		625 K	
Pressure (MPa)	Density (kg m ⁻³)	Viscosity (μPa s)	Density (kg m ⁻³)	Viscosity (μPa s)	Density (kg m ⁻³)	Viscosity (μPa s)
0.01	0.088406	15.494	0.085553	15.892	0.084868	15.989
0.05	0.44229	15.507	0.42798	15.906	0.42454	16.003
0.10	0.88521	15.523	0.85649	15.923	0.84960	16.020
0.15	1.3288	15.539	1.2855	15.940	1.2752	16.038
0.20	1.7730	15.555	1.7151	15.957	1.7012	16.055
0.25	2.2178	15.571	2.1452	15.974	2.1278	16.073
0.30	2.6632	15.588	2.5758	15.992	2.5549	16.090
0.35	3.1093	15.604	3.0070	16.009	2.9825	16.108
0.40	3.5561	15.621	3.4387	16.027	3.4106	16.126
0.50	4.4514	15.655	4.3036	16.062	4.2682	16.162
0.60	5.3492	15.689	5.1707	16.098	5.1279	16.199
0.80	7.1525	15.758	6.9109	16.172	6.8532	16.273
1.00	8.9656	15.829	8.6594	16.246	8.5863	16.348
1.50	13.542	16.015	13.066	16.440	12.953	16.544
2.00	18.179	16.211	17.522	16.643	17.366	16.749
2.50	22.875	16.418	22.026	16.856	21.825	16.963
3.00	27.629	16.635	26.577	17.078	26.328	17.187
3.50	32.439	16.862	31.171	17.309	30.872	17.418
4.00	37.304	17.100	35.808	17.548	35.456	17.659
5.00	47.185	17.604	45.199	18.052	44.734	18.163

TABLE 11. Viscosity of propane in the single phase regions—Continued

Temperature	600 K		620 K		625 K	
	Pressure (MPa)	Density (kg m ⁻³)	Viscosity (μPa s)	Density (kg m ⁻³)	Viscosity (μPa s)	Density (kg m ⁻³)
6.00	57.253	18.144	54.730	18.586	54.141	18.697
8.00	77.835	19.322	74.114	19.735	73.254	19.840
10.00	98.780	20.609	93.739	20.969	92.581	21.063
15.00	150.48	24.131	142.11	24.268	140.19	24.316
20.00	197.11	27.850	186.30	27.680	183.81	27.663
25.00	235.92	31.618	223.98	31.117	221.19	31.027
30.00	267.30	35.382	255.12	34.570	252.23	34.409
35.00	292.85	39.125	280.83	38.041	277.96	37.815
40.00	314.08	42.847	302.39	41.530	299.58	41.249
50.00	347.71	50.249	336.73	48.573	334.07	48.202
60.00	373.67	57.635	363.34	55.711	360.83	55.278
80.00	412.47	72.437	403.13	70.283	400.86	69.792
100.00	441.21	87.119	432.60	85.054	430.49	84.586

but it does not bring any real benefit for the viscosity surface representation: in fact for the present fluid the results of the initial density dependence analysis do not match the high accuracy reached by the proposed heuristic method.

8. Tabulations of the Overall Representation

Tables 10 and 11 report viscosity values of propane generated from the new Eq. (4), for both the saturation line and the single phase regions. The density values and the saturation properties are obtained from the fundamental equation of state of Span and Wagner⁶¹ for propane. These tables can also be used as reference values for the validation of a computer code.

The values in italics are calculated at conditions outside the validity limits of the equation given in Table 4 and then they have to be cautiously considered.

9. Conclusions

A new method based on the optimization of the functional form of multiparameter equations of state, set up by Setzmann and Wagner,²⁰ has been proposed for the development of viscosity equations and it has been applied to propane. The technique is completely correlative and directly based on the available viscosity data.

Considering the most reliable data sets, the new multiparameter viscosity equation shows an AAD value of 0.28%, with an improvement with respect to the conventional equation by Vogel *et al.*¹² considered as reference, whose AAD value is 0.76% for the same data base. The new method can be furthermore used as a powerful tool for experimental data screening. The optimization procedure by Setzmann and Wagner²⁰ is a promising tool for viscosity modeling; in fact

the equation developed through this technique is able to represent the whole viscosity surface well within the uncertainty of the experimental data.

As evidenced by Fig. 1, new experimental measurements should be required in order to fill the void inside the validity region of the equation, in particular for the vapor phase at low temperatures, for the liquid phase at low temperatures and moderate pressures, and for the region at high temperatures and pressures higher than the atmospheric value.

From the study of the behavior of the obtained viscosity equation a locus of minima on the viscosity surface has been found in the dense-gas region mostly at supercritical conditions. The locus of minima has been analytically represented.

The dilute-gas behavior of the present equation has been compared with the theoretically founded Rainwater–Friend model for the second viscosity virial coefficient and with experimental data in the low-density region, showing that even if the trend is not exactly matched, the quality of the equation is not at all influenced.

10. References

1. A. S. Teja and P. A. Thurner, Chem. Eng. Commun. **49**, 79 (1986).
2. B. Willman and A. S. Teja, Chem. Eng. J. **37**, 65 (1988).
3. K. J. Okeson and R. L. Rowley, Int. J. Thermophys. **12**, 119 (1991).
4. G. Scalabrin and M. Grigante, Proceedings 13th Symposium Thermo-physical Properties, Boulder, CO, 22–27 June 1997.
5. G. Cristofoli, M. Grigante, and G. Scalabrin, High Temp. - High Press. **33**, 83 (2001).
6. G. Scalabrin, G. Cristofoli, and M. Grigante, Int. J. Energy Res. **26**, 1 (2002).
7. J. F. Ely and H. J. M. Hanley, Ind. Eng. Chem. Fundam. **20**, 323 (1981).
8. M. L. Huber and J. F. Ely, Fluid Phase Equilib. **80**, 239 (1992).
9. S. A. Klein, M. O. McLinden, and A. Laesecke, Int. J. Refrig. **30**, 2089 (1997).
10. M. O. McLinden, S. A. Klein, E. W. Lemmon, and A. P. Peskin, NIST Standard Reference Database 23, Version 6.0, (REFPROP, 1998).
11. J. Millat, J. H. Dymond, and C. A. Nieto de Castro, *Transport Properties of Fluids. Their Correlation, Prediction and Estimation* (Cambridge University Press, Cambridge, 1996).
12. E. Vogel, C. Küchenmeister, E. Bich, and A. Laesecke, J. Phys. Chem.

- Ref. Data **27**, 947 (1998).
- ¹³ G. Scalabrin, P. Marchi, and R. Span, J. Phys. Chem. Ref. Data **35**, 839 (2006).
- ¹⁴ G. Scalabrin, C. Corbetti, and G. Cristofoli, Int. J. Thermophys. **22**, 1383 (2001).
- ¹⁵ G. Cristofoli, L. Piazza, and G. Scalabrin, Fluid Phase Equilib. **199**, 223 (2002).
- ¹⁶ G. Scalabrin, L. Piazza, and V. Vesovic, High Temp. - High Press. **34**, 457 (2002).
- ¹⁷ G. Scalabrin and G. Cristofoli, Int. J. Thermophys. **24**, 1241 (2003).
- ¹⁸ G. Scalabrin, G. Cristofoli, and D. Richon, Fluid Phase Equilib. **199**, 265 (2002).
- ¹⁹ G. Scalabrin, G. Cristofoli, and D. Richon, Fluid Phase Equilib. **199**, 281 (2002).
- ²⁰ U. Setzmann and W. Wagner, Int. J. Thermophys. **10**, 1103 (1989).
- ²¹ B. A. Younglove and J. F. Ely, J. Phys. Chem. Ref. Data **16**, 577 (1987).
- ²² P. J. Mohr and B. N. Taylor, Rev. Mod. Phys. **72**, 351 (2000).
- ²³ P. Becker, H. Bettin, H.-U. Danzebrink, M. Glaser, U. Kuetgens, A. Nicolaus, D. Schiel, P. De Bievre, S. Valkiers, and P. Taylor, Metrologia **40**, 271 (2003).
- ²⁴ S. E. Babb, Jr. and G. J. Scott, J. Chem. Phys. **40**, 3666 (1964).
- ²⁵ J. D. Baron, J. G. Roof, and F. W. Wells, J. Chem. Eng. Data **4**, 283 (1959).
- ²⁶ L. B. Bicher, Jr. and D. L. Katz, Ind. Eng. Chem. **35**, 754 (1943).
- ²⁷ L. T. Carmichael, V. M. Berry, and B. H. Sage, J. Chem. Eng. Data **9**, 411 (1964).
- ²⁸ D. E. Diller, J. Chem. Eng. Data **27**, 240 (1982).
- ²⁹ J. G. Giddings, J. T. F. Kao, and R. Kobayashi, J. Chem. Phys. **45**, 578 (1966).
- ³⁰ E. T. S. Huang, G. W. Swift, and F. Kurata, AIChE J. **12**, 932 (1966).
- ³¹ B. H. Sage and W. N. Lacey, Ind. Eng. Chem. **30**, 829 (1938).
- ³² A. S. Smith and G. G. Brown, Ind. Eng. Chem. **35**, 705 (1943).
- ³³ K. E. Starling, B. E. Eakin, and R. T. Ellington, AIChE J. **6**, 438 (1960).
- ³⁴ H. J. Strumpf, A. F. Collings, and C. J. Pings, J. Chem. Phys. **60**, 3109 (1974).
- ³⁵ G. W. Swift, A. J. Christy, and F. Kurata, AIChE J. **5**, 98 (1959).
- ³⁶ G. W. Swift, J. Lohrenz, and F. Kurata, AIChE J. **6**, 415 (1960).
- ³⁷ W. R. van Wijk, J. H. van der Veen, H. C. Brinkman, and W. A. Seeder, Physica (Amsterdam) **7**, 45 (1940).
- ³⁸ G. I. Galkov and S. F. Gerf, Zh. Tekh. Fiz. **11**, 613 (1941).
- ³⁹ S. F. Gerf and G. I. Galkov, Zh. Tekh. Fiz. **10**, 725 (1940).
- ⁴⁰ M. R. Lipkin, J. A. Davison, and S. S. Kurtz, Jr., Ind. Eng. Chem. **34**, 976 (1942).
- ⁴¹ Y. Abe, J. Kestin, H. E. Khalifa, and W. A. Wakeham, Physica A **93**, 155 (1978).
- ⁴² Y. Abe, J. Kestin, H. E. Khalifa, and W. A. Wakeham, Ber. Bunsenges. Phys. Chem. **83**, 271 (1979).
- ⁴³ H. Adzumi, Bull. Chem. Soc. Jpn. **12**, 199 (1937).
- ⁴⁴ E. W. Comings, B. J. Mayland, and R. S. Egly, Univ. Illinois Eng. Exptl. Sta. Bull. **354**, 1 (1944).
- ⁴⁵ M. Diaz Pena and J. A. R. Cheda, An. Quim. **71**, 34 (1975).
- ⁴⁶ M. Diaz Pena and J. A. R. Cheda, An. Quim. **71**, 257 (1975).
- ⁴⁷ J. J. Hurly, K. A. Gillis, J. B. Mehl, and M. R. Moldover, Int. J. Thermophys. **24**, 1441 (2003).
- ⁴⁸ J. Kestin, S. T. Ro, and W. A. Wakeham, Trans. Faraday Soc. **67**, 2308 (1971).
- ⁴⁹ J. Kestin, H. E. Khalifa, and W. A. Wakeham, J. Chem. Phys. **66**, 1132 (1977).
- ⁵⁰ A. Klemenc and W. Remi, Monatsch. Chem. **44**, 307 (1923).
- ⁵¹ J. D. Lambert, K. J. Cotton, M. W. Pailthorpe, A. M. Robinson, J. Scrivins, W. R. F. Vale, and R. M. Young, Philos. Trans. R. Soc. London, Ser. A **231**, 280 (1955).
- ⁵² K. Nagaoka, Y. Yamashita, Y. Tanaka, H. Kubota, and T. Makita, J. Chem. Eng. Jpn. **19**, 263 (1986).
- ⁵³ H. Senftleben and H. Gladish, Z. Phys. **125**, 653 (1949).
- ⁵⁴ T. Titani, Bull. Chem. Soc. Jpn. **5**, 98 (1930).
- ⁵⁵ M. Trautz and F. Kurz, Ann. Phys. **9**, 981 (1931).
- ⁵⁶ M. Trautz and K. G. Sorg, Ann. Phys. **10**, 81 (1931).
- ⁵⁷ E. Vogel, Int. J. Thermophys. **16**, 1335 (1995).
- ⁵⁸ J. Wilhelm and E. Vogel, J. Chem. Eng. Data **46**, 1467 (2001).
- ⁵⁹ R. Wobser and F. Müller, Kolloid Beihefte **52**, 165 (1941).
- ⁶⁰ J. V. Sengers, Int. J. Thermophys. **6**, 203 (1985).
- ⁶¹ R. Span and W. Wagner, Int. J. Thermophys. **24**, 41 (2003).
- ⁶² D. G. Friend and J. C. Rainwater, Chem. Phys. Lett. **107**, 590 (1984).
- ⁶³ J. C. Rainwater and D. G. Friend, Phys. Rev. A **36**, 4062 (1987).
- ⁶⁴ E. W. Lemmon and R. T. Jacobsen, Int. J. Thermophys. **25**, 21 (2004).